INVESTIGATION OF THE CURRENT DENSITY LIMITATIONS IN A THERMIONIC CONVERTER

BY COLEMAN KAPLAN

ANNUAL SUMMARY REPORT CONTRACT NONR 3738(00)

OFFICE OF NAVAL RESEARCH

MARCH 1963

REPORT NO. 25,081

THE MARQUARDT CORPORATION

AERO SPACE TECHNOLOGY RESEARCH OFFICE

THE Marquardt CORPORATION
16555 SATICOY STREET • VAN NUYS, CALIFORNIA • TELEPHONE 781 2121 • DTWX 213 781 0184 • CABLE MARQCOR

17 April 1963
Ref: 280/885-22/2672

Gentlemen:

A copy of Marquardt Report 25,081 on "Investigation of the Current Density Limitations in a Thermionic Converter" is enclosed. This is the Annual Summary Report for the period 1 March 1962 through 28 February 1963 on Contract Nonr 3738(00).

THE MARQUARDT CORPORATION

Thomas G Bek HKW
T. G. Bek, Manager
Van Nuys Contract Administration

RAL:TGB:ahd

Enclosure

21

OFFICE OF NAVAL RESEARCH
Contract Nonr 3738(00)
Task No. NR 099-366

Annual Summary Report

INVESTIGATION OF THE CURRENT DENSITY LIMITATIONS IN A THERMIONIC CONVERTER

by
Coleman Kaplan

ASTRO - The Marquardt Corporation
Van Nuys, California

March 1963

FOREWORD

This report has been prepared under Contract Nonr 3738-(00), Office of Naval Research, and covers the period from March 1, 1962 to February 28, 1963. The work performed under this contract was under the technical supervision of Commander J. J. Connelly, Jr., of ONR, and Dr. R. A. Laubenstein of Marquardt; their interest, encouragement, and guidance are gratefully acknowledged.

The author wishes to acknowledge the capable assistance of N. N. Hankin and J. B. Merzenich in the experimental aspects of the work reported herein. The diodes used in these experiments were fabricated under the supervision of J. R. Peterson, who also participated in the design of these test cells. The special test circuits used in this program were designed and assembled by J. B. Merzenich. In addition, helpful discussions with W. E. Beyermann and Dr. R. A. Laubenstein are gratefully acknowledged.

Approved By:

Richard A. Laubenstein
Principal Research Scientist
Power Conversion Research

Arthur N. Thomas
Chief Research Scientist
Advanced Projects

FOREWORD

This report has been prepared under Contract Nonr 3738-(00), Office of Naval Research, and covers the period from March 1, 1962 to February 28, 1963. The work performed under this contract was under the technical supervision of Commander J. J. Connelly, Jr., of ONR, and Dr. R. A. Laubenstein of Marquardt; their interest, encouragement, and guidance are gratefully acknowledged.

The author wishes to acknowledge the capable assistance of N. N. Hankin and J. B. Merzenich in the experimental aspects of the work reported herein. The diodes used in these experiments were fabricated under the supervision of J. R. Peterson, who also participated in the design of these test cells. The special test circuits used in this program were designed and assembled by J. B. Merzenich. In addition, helpful discussions with W. E. Beyermann and Dr. R. A. Laubenstein are gratefully acknowledged.

Approved By:

Richard A. Laubenstein
Principal Research Scientist
Power Conversion Research

A. N. Thomas
Arthur N. Thomas
Chief Research Scientist
Advanced Projects

ABSTRACT

Oscillations in grid voltage, output voltage and output current were observed over a wide range of operating conditions with a cesium-vapor triode. At higher cesium pressures, the oscillation period is an increasing function of the cesium pressure, which implies that the oscillations are controlled by scattering of positive ions in the interelectrode region. An approximate calculation of the ion accelerating voltage required to transfer ions from the middle of the emitter-collector space to the collector indicates a voltage of between 0.5 and 1.0 volt. This calculation is based on collisionless ion transport at low cesium pressures and ion transport dominated by charge-exchange collisions at high cesium pressures. It was observed that the oscillations stop at a definite point on the current-voltage characteristic.

Pulsed-discharge experiments were initiated to investigate current-density limiting factors in a cesium diode operating in the intermediate temperature range. The experimental technique consisted of applying a pulsed discharge to the test cell and observing the effect upon output current after the pulse. When the diode operation was space-charge limited, a large increase in current was observed after the pulse; whereas if the current was nearly emission limited, only a small increase was observed. Reasonable agreement was obtained between the current density measured after a pulsed discharge and the saturated electron current density obtained from the literature. Measurements of the time required to establish equilibrium after the pulsed discharge provided information on the physics of cesium diode thermionic converters. A calculation based upon the experimental measurements indicates that charge-exchange collisions will control ion transport to the emitter or collector, where surface recombination will occur.

Calculations have been performed based upon a literature survey of charge exchange collisions and ion mobility in cesium vapor. Charge exchange collisions result in a slowing down of positive-charge transfer within or across the interelectrode volume. The exploratory measurements of this report, together with the calculations summarized in Appendix A, indicate that charge exchange collisions may play an important part in determining the current-limiting factors in cesium thermionic converters.

TABLE OF CONTENTS

LIST OF FIGURES

I. INTRODUCTION

The purpose of the work summarized in this report is to obtain a better understanding of the factors which limit the current density in a cesium-diode thermionic converter operating in the emitter temperature range of 1270 to 1900°C. For maximum power output, it is desirable to operate the converter with an output voltage approximately equal to the difference between the emitter and collector work functions. If complete space-charge neutralization could be attained, together with negligible resistance in the interelectrode plasma, then the output current would be equal to the emission-limited current at the emitter surface. The chief question under investigation in this program is: In an actual thermionic converter, what factors limit the current density to less than the theoretical emission-limited value?

Conceptually, the simplest mode of converter operation utilizes a high-work-function emitter operating at a high surface temperature[1]. Neutral cesium atoms reach the emitter surface and are emitted as cesium ions in a quantity sufficient to neutralize the electron space charge. The cesium pressure is maintained sufficiently low so that the mean free path for elastic scattering of electrons is of the order of or greater than the spacing between emitter and collector. Then the component of plasma resistance due to scattering of electrons by neutrals is negligible. The spacing is small enough so that the resistance due to electron-ion collisions is also small. The cesium coverage of the emitter surface is usually negligible. Under these conditions, the output current can approach the emission-limited current of the emitter. However, a high emitter temperature is required for this mode of operation, leading to short operating lifetime and serious difficulties in converter and heat-source materials.

A lower temperature range of cesium diode operation is available, using emitter temperatures from 1270°C to 1900°C. For this range of operation, the effective emitter work function should be less than the ionization potential of cesium, in order to obtain reasonable current density and efficiency. Emitter materials of current interest include cesium-coated refractory metals, dispenser materials such as thoriated tungsten, and various metallic carbides. Cesium ions can be obtained by both volume and surface ionization. Operation in this temperature range is more complex and is less well understood than operation at high emitter temperature and low cesium pressure.

There are several factors which decrease the output current to less than the emission-limited current in the intermediate temperature range of cesium diode operation. Complete neutralization of the electron space charge may not be realized, so that a space-charge barrier is present between the emitter and collector surfaces. Electron scattering can cause appreciable resistance in the interelectrode plasma, decreasing the output current at a given voltage. In some cases, oscillations in output current (and voltage) yield a decrease in the average current and power density. The emission limited current in itself is an uncertain factor in that it can be affected by many parameters of converter operation, including the presence of a positive ion sheath near the emitter.

Background information for this program was obtained under the Marquardt Corporate Independent Research Program on the transient characteristics of a low-temperature cesium diode[2]. This program suggested the use of pulse-discharge techniques to explore output-current-limiting mechanisms in the intermediate-temperature thermionic converter for the present program. Oscillations in the frequency range of 10 to 30 kc were also observed with the low-temperature cesium diode. In part, these observations provided the foundation for the measurement of oscillations in the 592 triode reported herein.

II. SUMMARY

Experiments were conducted with a cesium-vapor triode. Oscillations in grid voltage, output voltage and output current were observed over a wide range of operating conditions. At higher cesium pressures, the oscillation period is an increasing function of the cesium pressure, which implies that the oscillations are controlled by scattering of positive ions in the interelectrode region.

An approximate calculation of the ion accelerating voltage required to transfer ions from the middle of the emitter-collector space to the collector indicates a voltage of between 0.5 and 1.0 volt. This calculation is based on collisionless ion transport at low cesium pressures and ion transport dominated by charge-exchange collisions at high cesium pressures. This voltage is consistent with the sheath potential which might be expected in a cesium plasma with alternating negative and positive charge density.

It was observed that the oscillations stop at a definite point on the current-voltage characteristic. There is some evidence that the current at the cessation of oscillations corresponds to the zero-field saturated emission of the thoriated-tungsten emitter; however, a further increase in current is observed when the output voltage is lowered. An increase in current beyond the zero-field saturated current could be due to field-enhanced emission caused by a voltage gradient across the emitter sheath.

Based upon preliminary experiments done under the Marquardt Corporate Independent Research Program, pulsed-discharge experiments were initiated to investigate current-density limiting factors in a cesium diode operating in the intermediate temperature range. The experimental technique consisted of applying a pulsed discharge to the test cell and observing the effect upon output current after the pulse. When the diode operation was space-charge limited, a large increase in current was observed after the pulse; whereas if the current was nearly emission limited, only a small increase was observed. Reasonable agreement was obtained between the current density measured after a pulsed discharge and the saturated electron current density obtained from the literature.

Measurements of the time required to establish equilibrium after the pulsed discharge provided information on the physics of cesium diode thermionic converters. Based upon the measured time constant of the exponential current decay, an estimate of the potential in the interelectrode region was obtained. The calculation indicates that the interelectrode region is at a potential of about +0.6 volt with respect to the top of the work function barrier at the emitter or collector. This voltage could be maintained by a slight excess of positive ions over electrons in the interelectrode region. The positive ions would be supplied by volume ionization; charge-exchange collisions will control ion transport to the emitter or collector, where surface recombination will occur.

Appendix A contains calculations based upon a literature survey of charge exchange collisions and ion mobility in cesium vapor. Charge exchange collisions result in a slowing down of positive-charge transfer within or across the inter-electrode volume. The exploratory measurements of this report, together with the calculations summarized in Appendix A, indicate that charge exchange collisions may play an important part in determining the current-limiting factors in cesium thermionic converters. Further quantitative work is required to obtain a better understanding of the importance of this factor.

III. CONCLUSIONS

1. Coherent oscillations can occur in a cesium discharge under either collision-free or collision-dominated conditions. At sufficiently high cesium pressures the oscillation frequency is inversely proportional to the cesium pressure.

2. The observed variation in oscillation frequency with cesium pressure is consistent with a physical picture based on ion mobility determined by charge exchange collisions.

3. Pulsed discharge experiments provide a useful technique for investigating current-limiting factors in thermionic converters.

4. At emitter temperatures of 1270 to 1300°C and a cesium pressure of 2.7 torr, the output current obtained from a cesium diode is highly space-charge limited. At a lower cesium pressure of 1 torr, the limitation is less severe.

5. After a pulsed discharge is applied to a converter, the output current decays exponentially. The observed decay time is compatible with an interelectrode-space potential of +0.6 V (calculated from the charge-exchange cross section) with respect to the top of the emitter or collector work-function barriers.

6. Consideration of the cross section for charge-exchange collisions between cesium ions and cesium atoms, and the resultant ion mobility, indicates that this collision process can be very important in the theory and operation of the cesium diode.

IV. OSCILLATIONS AND THEIR RELATION TO ELECTRON CURRENT AND ION MOBILITY

A. Experimental Tube

The tube used in the experiments is a modified Eimac 592 triode. This is a glass-envelope transmitting tube with a directly-heated thoriated-tungsten emitter. The tube was modified by adding a suitable tubulation for the introduction of cesium, and by cutting a hole in the collector (plate) to allow measurement of the emitter temperature with an optical pyrometer. The 0.3 mm filament wire is coiled into a 5.5 mm OD helix; the 8.8 mm ID grid and the 22 mm ID collector cylinder are both concentric with this emitter structure. The total surface area of the emitter wire is 0.77 cm^2.

B. Experimental Procedure

Cesium was introduced and the tube was sealed and placed in an oven for maintaining the desired cesium pressure. The sealed-off end of the exhaust tubulation was used as a cesium reservoir, and the tube wall was maintained above the cesium condensation temperature. The filament was heated with 60 cps half-wave-rectified current. Pulsed grid voltage, output voltage and output current measurements were made with an oscilloscope during the off portion of the heating cycle (to eliminate errors caused by the heating voltage). The emitter temperature was measured with an optical pyrometer and corrected for the filament emissivity.

C. Experimental Results

1. Oscillation Frequency

Large-scale coherent oscillations in output voltage and current were observed over a wide range of operating conditions. Typical oscillations are shown in Figure 1 for a cesium pressure of about 8×10^{-3} torr. During the measurement pulse, the output voltage oscillates between +0.5 and -1.0 volt, while the output current varies between 0.4 and 0.25 A. Oscillations in the floating grid potential are also shown.

Two distinct oscillation frequencies are clearly visible in this oscilloscope photograph. The higher frequency of approximately 100 kc is believed due to positive ion oscillations between the emitter and the grid, and the lower frequency oscillations of 10 kc may be due to similar oscillations between the emitter and collector. It can be noted that the higher frequency is predominant in the grid voltage trace, and the lower frequency predominates the output voltage trace.

An oscilloscope photograph of the oscillations observed at a higher cesium pressure of 5×10^{-2} torr is shown in Figure 2. It can be seen that the low and high frequency oscillations occur at 2.5 kc and 60 kc respectively. As before, the high frequency oscillations are more apparent in the grid voltage trace and the low frequency oscillations are predominant in the output voltage trace.

OSCILLATIONS IN OUTPUT VOLTAGE, GRID VOLTAGE, AND OUTPUT CURRENT

CESIUM TEMPERATURE = 150°C
CESIUM PRESSURE = 8×10^{-3} torr
EMITTER TEMPERATURE = 1725°C

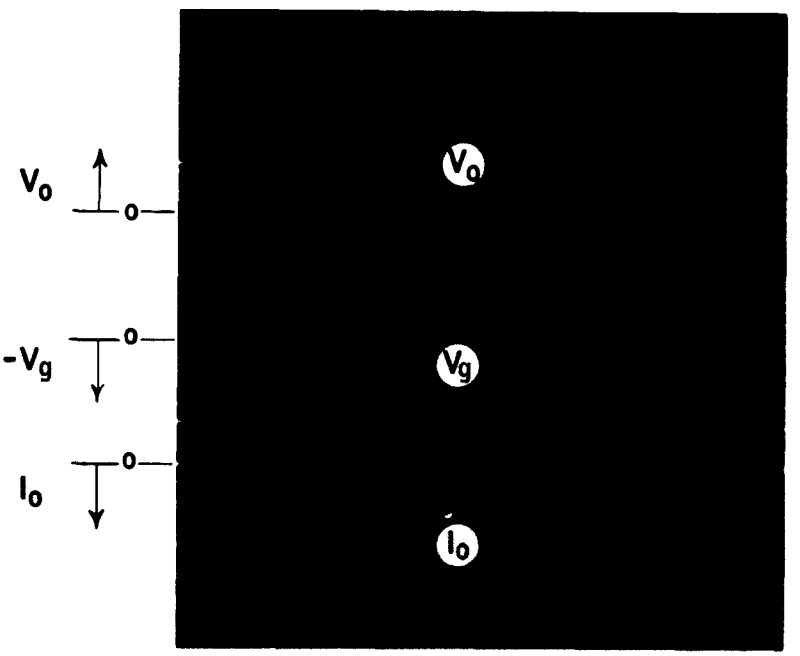

UPPER TRACE: OUTPUT VOLTAGE, 1 volt/division

MIDDLE TRACE: GRID VOLTAGE (REFERENCED TO EMITTER), 0.5 volt/division

LOWER TRACE: OUTPUT CURRENT, 0.5 A/division

HORIZONTAL SCALE: TIME, 10^{-4} second/division

OSCILLATIONS IN OUTPUT VOLTAGE GRID VOLTAGE, AND OUTPUT CURRENT WITH INCREASED CESIUM PRESSURE

CESIUM TEMPERATURE = 188°C
CESIUM PRESSURE = 5×10^{-2} torr
EMITTER TEMPERATURE = 1725°C

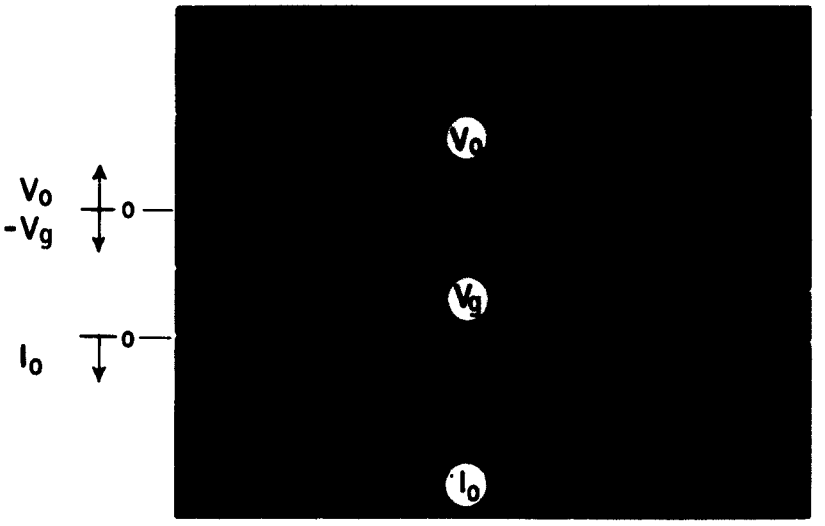

UPPER TRACE: OUTPUT VOLTAGE, 0.5 volt/division

MIDDLE TRACE: GRID VOLTAGE (REFERENCED TO EMITTER), 0.5 volt/division

LOWER TRACE: OUTPUT CURRENT, 2 A/division

HORIZONTAL SCALE: TIME, 2×10^{-4} second/division

R-13,300

Figure 2

The oscillation period and frequency (for the lower-frequency oscillations) are shown as a function of cesium pressure in Figure 3. Measurements were made at the onset of oscillations; i.e., at the lowest current at which a coherent oscillation was obtained. These measurements were taken at an emitter temperature of 1805°C. No significant variation in oscillation frequency was observed when the emitter temperature was changed, provided the convention of taking the measurements at the onset of oscillations is observed. Increasing the current beyond the minimum level for oscillations caused a decrease in the oscillation frequency.

At the low-pressure end of the curve, from A to B, the oscillation period is nearly constant at 10^{-5} seconds, corresponding to an oscillation frequency of 100 kc. In the middle section of the curve, from B to C, the oscillation period is approximately proportional to the one-third power of the cesium pressure ($t \propto p^{1/3}$), and in the higher- pressure portion of the curve, from C to D, the oscillation period is directly proportional to the cesium pressure ($t \propto p$).

The temperature of the cesium gas in the region between the emitter and the collector is nearly constant, so that the cesium atom density is proportional to the pressure. Therefore, the oscillation period between points C and D is approximately proportional to the cesium density. This dependence implies that the period is controlled by scattering of positive ions and/or electrons in the inter-electrode region at the higher cesium pressures. At lower cesium pressures the scattering is negligible and the oscillation period appears to be a function of the transport time of charged particles in the interelectrode region. The middle section of the curve from B to C may represent a transition region between these two regimes.

2. Current-Voltage Characteristics

Figure 4 shows the current-voltage characteristics obtained at a cesium pressure of 8×10^{-3} torr. Curves are shown for several different values of emitter temperature. The measurements were taken during the off-portion of the heating cycle. The open-circuit grid voltage (floating grid potential) is shown as a parameter on the current-voltage characteristics. It can be seen in Figure 4 that oscillations started at positive output voltage and extended over an appreciable portion of each current-voltage characteristic. As the output current was increased, a point on each characteristic was reached where the oscillations suddenly ceased and steady voltage and current were again obtained.

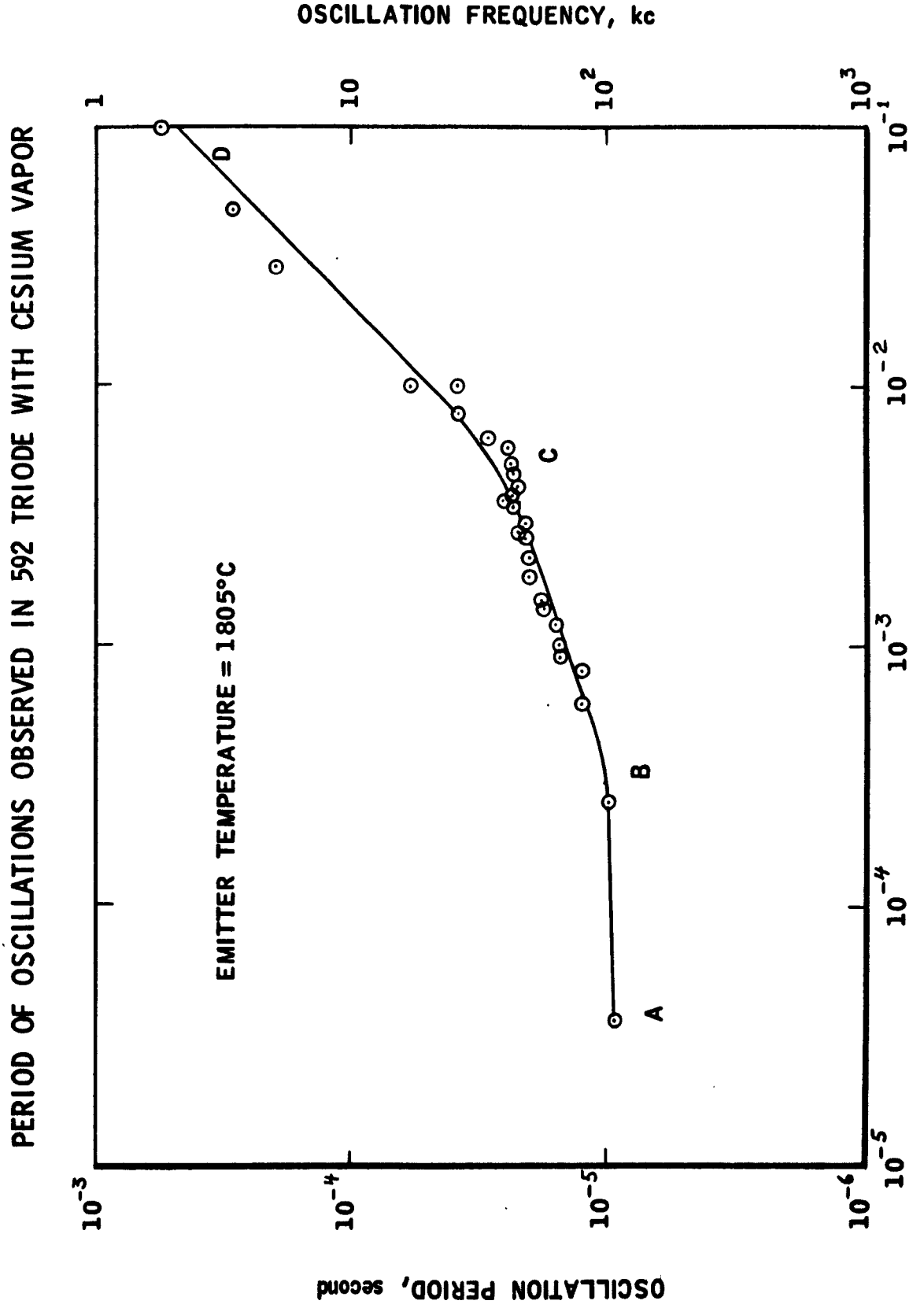
PERIOD OF OSCILLATIONS OBSERVED IN 592 TRIODE WITH CESIUM VAPOR
EMITTER TEMPERATURE = 1805°C
OSCILLATION FREQUENCY, kc
1
10
10^2
10^3
10^{-1}
10^{-2}
10^{-3}
10^{-4}
10^{-5}
10^{-6}
A
B
C
D
OSCILLATION PERIOD, second
CESIUM PRESSURE, torr

Figure 3

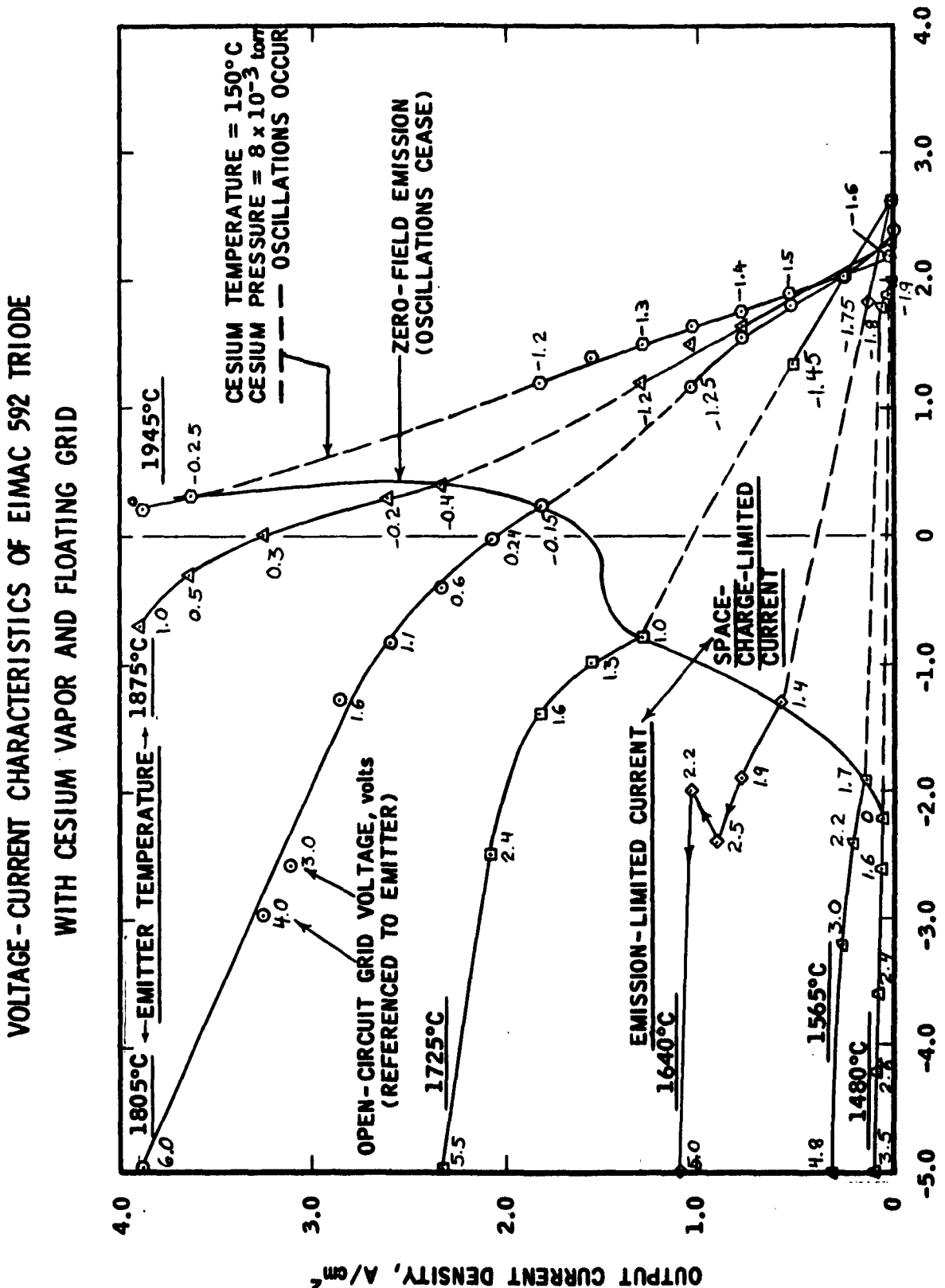

R-13,296A

Figure 4

D. Discussion and Interpretation of Data

1. Physical Mechanism of Observed Oscillations

Instabilities in the operation of a gaseous discharge in cesium vapor have been experimentally observed by many workers[3-5]. These instabilities often lead to coherent oscillations in voltage and current. In the analysis of the oscillations, it is usually assumed that space-charge effects are the most important physical mechanisms involved, although wave phenomena such as ion-wave instabilities[6] may play a part in triggering the oscillation. Space-charge oscillations appear to be consistent with the oscillation frequencies observed with the 592 triode.

Calculations of the potential distribution across a plasma diode indicate that more than one potential profile is possible for a given set of boundary conditions[7]. In some cases, no stable potential distribution exists. The calculation by Hernqvist and Eichenbaum[8] indicates that instabilities arise in a collisionless plasma when the space-charge is nearly neutralized. Their results yield a double-valued solution for the potential distribution when the electron and ion emission currents are such as to produce a plasma that is nearly neutral. Their calculation is for a collisionless plasma; in the 592 triode the plasma is essentially collisionless at lower cesium pressures and is collision-dominated at higher cesium pressures.

Space-charge oscillations require the alternate buildup and decay of an ion surplus in the interelectrode region. An excess of ions in the interelectrode region causes an increase in electron current from the emitter together with a decrease in the emitted ion current. The resulting potential distribution eventually yields a negative space potential with a barrier which limits the electron emission to a value below the saturation value. In this type of oscillation, we would expect the oscillation frequency to be closely related to the ion transit time within or across the interelectrode region.

Order-of-magnitude estimates can be obtained of the ion-accelerating voltage, V, required to transfer ions from the middle of the emitter-collector space to the collector, where surface recombination will occur. The oscillation period t is shown in Figure 3; the ion transit time will be estimated as 1/2 of the oscillation period. The average distance covered by an ion during this transit time is of the order of 1/2 of the emitter-collector spacing of $w = 0.84$ cm, so that the average ion velocity can be approximated as $w/t = 0.84/t$ cm per sec.

A minimum value of the ion-accelerating voltage (when no ion-scattering collisions occur) is given by the energy relation

$$eV = 1/2\ mv^2 = \frac{mw^2}{2t^2}.$$

The voltage calculated from this equation is plotted as a function of cesium pressure on the left side of Figure 5. The accelerating voltage calculated in this manner is only applicable if the ion mean free path is larger than the interelectrode spacing, so that ions do not lose energy by scattering collisions during transport to the collector.

The most probable collision process for low-energy cesium ions is the charge-exchange collision, which results in a slowing down of charge transfer across the cesium plasma (see Appendix A). The mean free path for this process is given in terms of the average atom cross-section $\bar{Q}$ ($\approx 2 \times 10^{-13}$ cm^2 for charge-exchange collisions) and the average atom density $\bar{N}$ as

$$\lambda = \frac{1}{\bar{N}\bar{Q}}.$$

The mean free path is equal to the spacing, 0.84 cm, at an atom density of $\bar{N} = 6 \times 10^{12}$ atom per cm^2, which corresponds to a cesium pressure of 3×10^{-4} torr. At higher cesium pressures than this, the ion collides many times during transport to the collector and an equilibrium ion velocity is very soon established. This equilibrium velocity is given by the mobility relation

$$v = \mu E$$

which can be written as

$$\Delta V = \frac{v\,\Delta x}{\mu}$$

if the actual electric field E is approximated by a linear one equal to $\Delta V/\Delta x$, where $\Delta x = w/2$. Using the same approximation for the ion velocity as before, $v = w/t$, the ion accelerating voltage required for the observed oscillation period becomes

$$V = \frac{w^2}{2\mu t}.$$

The mobility is given in Appendix A as

$$\mu = \frac{3.06\sqrt{T_g}}{p}$$

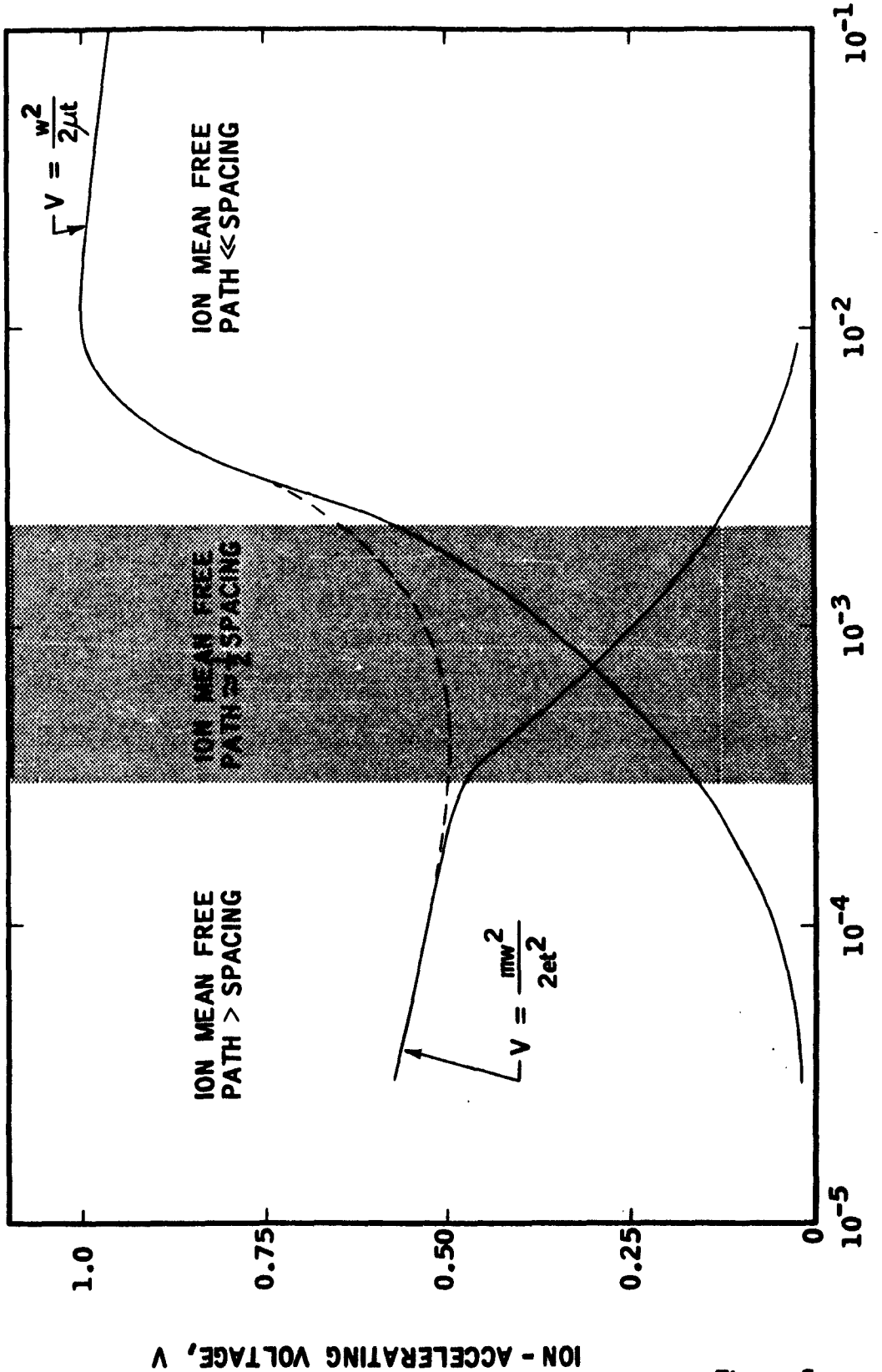

Figure 5

R-14.805

The gas temperature T_g is estimated as 100°K above the cesium condensation temperature (this is the approximate collector and tube wall temperature) to calculate the mobility as a function of cesium pressure. The ion-accelerating voltage calculated in this manner is shown on the right hand side of Figure 5.

There are three regions indicated in Figure 5. At low cesium pressures the accelerating voltage is determined by dynamical considerations, since the collision probability is very small. At high cesium pressures the voltage is determined by collision processes, and can be calculated from the mobility equation. In the intermediate pressure range the required voltage will be larger than the accelerating voltage given by either the mobility considerations or the dynamical relation alone. An accelerating voltage something like the dashed curve is expected in this region.

Examination of Figure 5 indicates that the required ion-accelerating voltage will always be larger than the thermal energy of ions in equilibrium with the cesium gas, which is less than 0.1 eV. The voltages of 0.5 to 1.0 volt are consistent with the fluctuations in output voltage and grid voltage indicated by the experimental observations. The magnitude of these voltages is also consistent with the sheath potential which might be expected in a cesium plasma with alternating negative and positive charge density.

Oscillations were observed by Luke and Jamerson[9] in a diode under conditions roughly similar to those in the 592 triode. Their tube had a 0.010 inch thoriated-tungsten filament emitter and a cylindrical collector. Three different collector diameters were used; 0.102 inch, 0.218 inch, and 0.437 inch. Oscillations were observed with the larger-diameter collector over a wide range of emitter temperature, in agreement with the results presented here. Luke and Jamerson reported that the oscillation frequency is roughly proportional to the square of the collector diameter and therefore proportional to the square of the emitter-collector spacing. This is in agreement with the mobility equation, which indicates that the period is proportional to the square of the spacing at constant accelerating voltage.

Other workers using plane-parallel geometry and close spacing report that the oscillation period is directly proportional to the electrode spacing[4]. If the ion-accelerating voltage is constant, this is in agreement with the dynamical relation, which would be expected to apply when the spacing becomes less than the mean free path for charge-exchange collisions.

Oscillations were observed by Carabateas and Koskinen[10] in a cesium filled tube with geometry similar to the 592 triode, except that no grid was present. Their measurements indicate oscillations over a range of cesium pressure from 10^{-6} to about 5×10^{-3} torr, and show a decreasing period (increasing frequency) with increasing cesium pressure. Our measurements indicate that the oscillation period increases with increasing cesium pressure. The reason for this discrepancy is not apparent at the present time. A possible explanation is that their device employed a niobium emitter, whereas the 592 triode has a thoriated-tungsten emitter. The different emitter materials will provide a different ratio of ion-to-electron emission. This difference may result in a different mechanism for the oscillations.

2. Grid Voltage and Changes in Plasma Potential

The open-circuit voltage between the grid and the emitter was measured at each point where output voltage and current measurements were taken. The grid voltage is shown as a parameter on the output voltage-current characteristics in Figure 4. The sign convention used in this figure for the grid voltage gives the grid voltage with respect to the emitter.

Attempts were made to measure the grid voltage-current characteristic in order to obtain the plasma potential via the usual Langmuir probe characteristic. It was found that at zero or positive grid bias the grid current was too high to allow use of the grid as a Langmuir probe. This is believed due to the large grid area, compared to the area of probes normally used in gaseous discharges. However, drawing fairly high grid current caused only a small change in the output voltage and current.

The open circuit grid voltage should follow the plasma potential at the grid location (1.7 mm from the emitter) quite closely, so that a change in open circuit grid voltage should indicate a corresponding change in the plasma potential.

In the retarding portion of the current-voltage characteristics, ranging from the open-circuit voltage to the onset of oscillations, the change in grid voltage is less than the change in output voltage. The grid voltages in this region are shown on the 1945°C curve to illustrate this. A change of 1 volt in the output voltage, going from 2.2 volts open-circuit to 1.2 volts at the onset of oscillations, yields a change in grid voltage of 0.4 volt. This indicates that, in the retarding portion of the curve, the major part of the voltage change between the emitter and collector occurs across either the collector sheath or the bulk of the inter-electrode plasma.

This observation agrees with previous measurements by Shaver(11). Shaver made pulsed Langmuir-probe measurements in a cesium plasma diode consisting of a tungsten emitter and a concentric nickel collector. He observed that the probe floating potential and the apparent plasma potential were not strongly dependent upon the value of the collector voltage for collector voltages between -1 and -4 volts.

In the portion of the current-voltage characteristic just after the cessation of oscillations, the grid voltage changes more than the output voltage does, indicating a shift in plasma potential in the vicinity of the emitter. Toward the higher negative-voltage portion of the characteristic, the plasma potential appears to follow the output voltage quite closely, indicating that the applied voltage is appearing across a sheath at the emitter. This sheath voltage should be capable of lowering the work function barrier at the emitter-plasma interface, which would increase the output current to values larger than the zero-field emission. The voltage applied across the very narrow emitter sheath can yield a high electric field at the emitter surface. It is quite possible that we are dealing with a patchy emitting surface, and that the sheath thickness is comparable to the patch dimension, which then yields an anamolous behavior, sometimes referred to as the "anamolous Schottky effect". This is further complicated by the possibility that the sheath thickness can vary with the magnitude of the applied voltage.

3. Relation of Oscillations to Saturated Electron Emission

Current-voltage characteristics are shown for various emitter temperatures in Figure 6 . At all temperatures for which data were taken, large-scale oscillations in output voltage and current were observed over a portion of the characteristic. When the current is increased past a definite and reproducible point on the characteristic, the oscillation amplitude drops very sharply to essentially zero. The sudden cessation of oscillations observed in the 592 triode led to the speculation that the current at this point is closely related to the zero-field saturated electron emission current.

Waymouth indicates that the cessation of oscillations is a measure of the saturation emission current in fluorescent lamp tubes(12). This is based on a negative space-charge potential well near the emitter surface such that positive-ion oscillations in this negative well cause oscillations in the voltage and current. When saturated emission current is drawn from the emitter this negative potential well no longer exists and the oscillations cease.

This technique of using oscillations to measure saturation emission currents was used by Zollweg and Gottlieb to measure the saturated emission in a cesium diode[4]. They obtained good agreement between the saturation current measured from oscillations and the saturation current measured by examination of the slope of the output current as a function of the output voltage. However, Houston[5] points out that over at least part of the experimental range covered by Zollweg and Gottlieb the ion current was many times larger than that required for space charge neutralization of the electron current, so that a stable negative potential well near the emitter surface is not possible.

The current density at the cessation of oscillations in the 592 triode is plotted in Figure 6 as a function of the emitter temperature. The work function ϕ that corresponds to the observed current density can be calculated from the emission equation

$$J = 120\ T^2 \exp\ (-11{,}610\ \phi/T)$$

This "effective work function" is shown in Figure 6. For purposes of comparison the vacuum work function of thoriated tungsten[13] is also shown. In addition, the effective work function calculated from the output current density obtained by Houston for a thoriated tungsten cesium diode operating under short-circuit conditions[5] is shown. It can be seen that the effective work function obtained from our oscillation data is lower than that obtained from Houston's data and is between 0.2 and 0.3 eV higher than the vacuum work function of thoriated tungsten. It is not expected that the presence of cesium near the emitter would raise its work function; however, the thoriated tungsten filament used in this experiment was probably not completely activated.

If we assume that the work function calculated from the current density for cessation of oscillations represents the true zero-field work function of the emitter surface, then we can calculate the positive ion current from the Saha-Langmuir equation.

$$J^+ = \frac{p/\sqrt{2\pi m^* k T_g}}{1 + 2 \exp\left[\frac{e(V_i - \phi)}{k\ T_E}\right]}$$

In addition, if we assume that the maximum space-charge-neutralized electron current density is given in terms of this ion current density by the relation

$$\frac{J^-}{J^+} = \sqrt{\frac{m^+}{m^-}} = 492$$

CURRENT DENSITY AND EFFECTIVE WORK FUNCTION OF 592 TRIODE AT CESSATION OF OSCILLATIONS

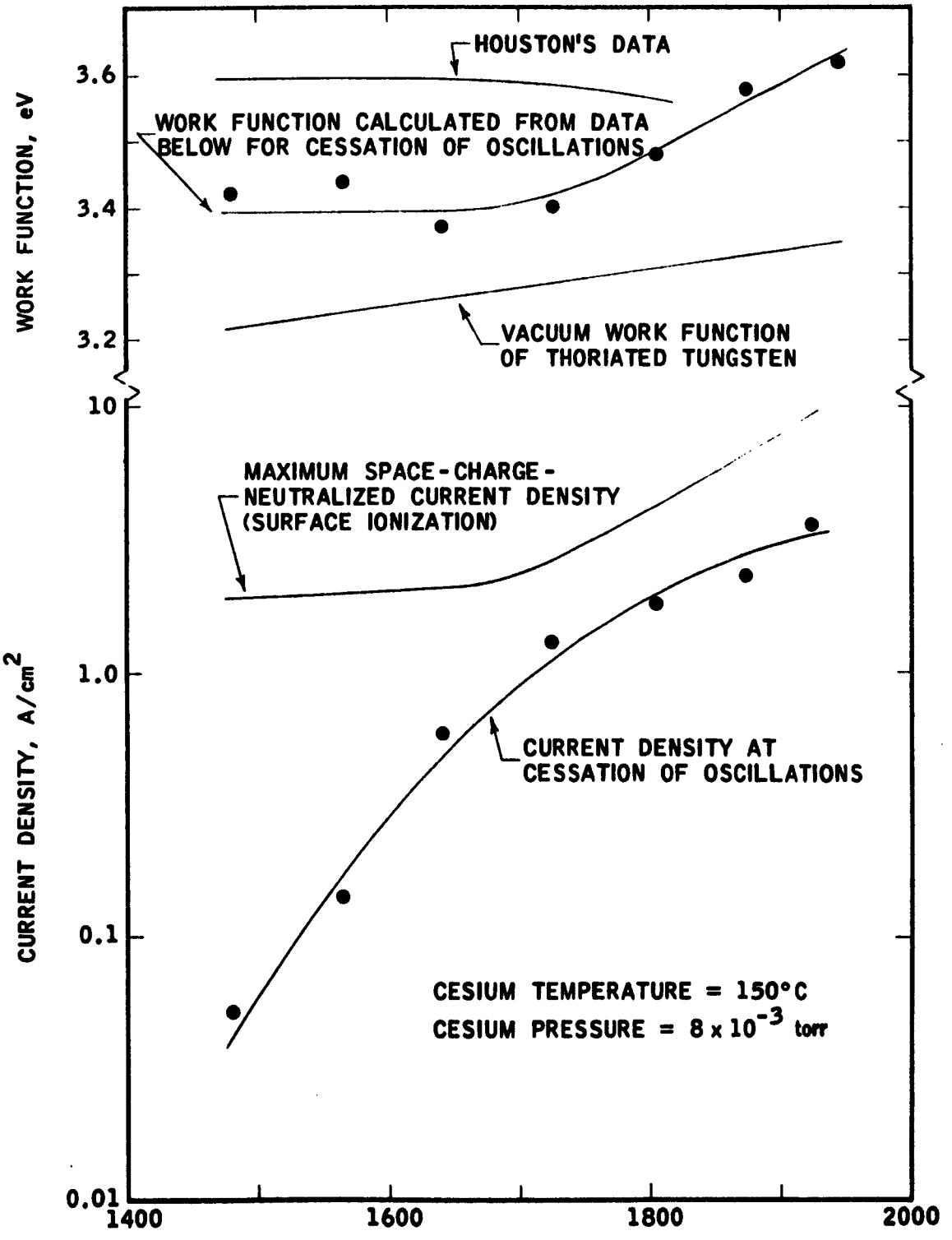

R-14,661

Figure 6

then we can calculate this electron current density. The result of these calculations, using the work functions from the oscillation data, is shown in Figure 6.

Comparison of this space-charge-neutralized current density curve with the actual current density at the cessation of oscillations in Figure 6 indicates that it is unlikely that the electron current was space-charge-limited during oscillations. This observation is not compatible with the physical picture of a negative space-charge potential well with positive ion oscillations as proposed by Waymouth[12] or by Zollweg and Gottlieb[4]. Therefore, there is not a clear-cut relation between the cessation of oscillations and saturated electron emission in the 592 triode and in other thermionic converters.

Examination of the voltage-current characteristics indicates that in some cases the current density increases rapidly after the cessation of oscillations. This large increase for relatively small changes in output voltage may mean that the oscillations stop before zero-field saturated emission is reached, or that it may mean that the increased current is field-enhanced because of the anamolous Schottky effect mentioned in the preceding section.

V. PULSED-DISCHARGE MEASUREMENTS

A. General Approach

Background information for this portion of the program was obtained under the Marquardt Corporate Independent Research Program[2, 14]. A study was performed on a low-temperature cesium diode with an oxide-type emitter. A short (sub-microsecond) pulse was applied to this diode to create positive ions. It was observed that these ions were effective in neutralizing the electron space charge, and electron currents after the pulse were observed which were up to 100 times larger than the steady-state space-charge-limited current. The diode current after the pulse showed an exponential decay with a time constant which varied from about 5 microseconds at 10^{-3} torr, to 100 microseconds at 0.3 torr.

The purpose of the pulsed-discharge experiments performed under this program is to determine the feasibility of and establish criteria for the use of transient-measurement techniques to investigate current-density limiting factors in an intermediate temperature cesium diode. The experimental technique consists of applying a pulsed discharge to the test cell and observing the effect on the output current after the pulse is fired. This provides a measurement of the emission-limited current, since positive ions resulting from the pulsed discharge can be used to neutralize the electron current after the pulse. If the diode operation is space-charge-limited, then a large increase in current is observed after the pulse; whereas, if the current is nearly emission limited, then only a small increase is observed. In addition, measurements of the time required to establish equilibrium conditions after a pulsed discharge provides information on the basic physical mechanisms involved in thermionic converter operation.

B. Experimental Equipment

1. PlD Test Cell

A PlD (plane-parallel geometry, 1.25 cm^2 emitter area diode) cesium thermionic converter has been fabricated for this program. This converter is shown in Figure 7. The emitter and collector electrodes are molybdenum, and the electrode spacing can be changed during converter operation. The emitter is heated by electron bombardment from a thoriated tungsten filament. The configuration of this test cell facilitates transient measurements; coaxial current and potential leads (not shown in photograph) are used.

PID THERMIONIC CONVERTER TEST CELL

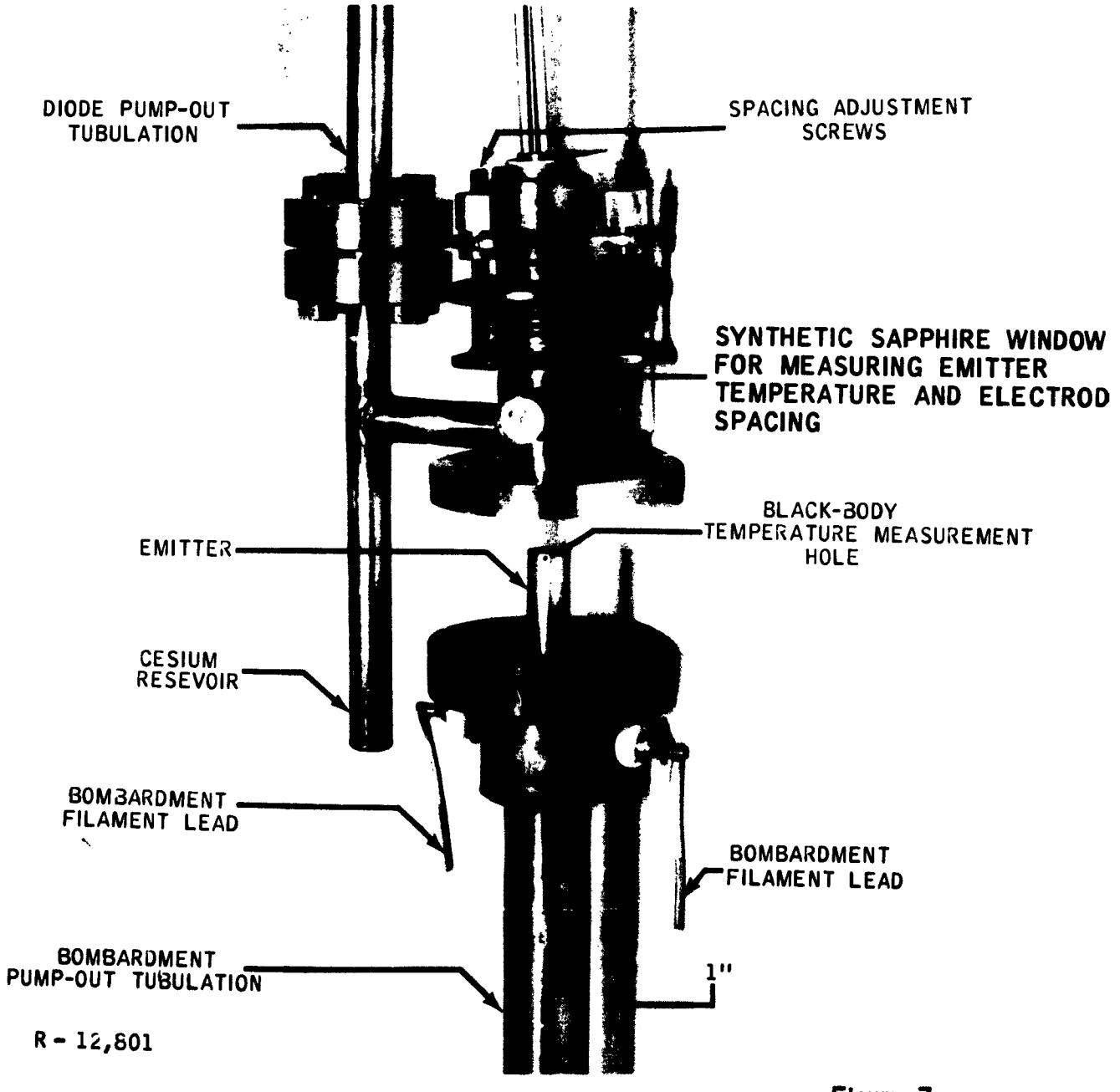

Figure 7

2. P11D Test Cell

During the latter part of the contract year, some pulsed-discharge experiments were performed on the P11D (plane parallel geometry, 11.4 cm^2 emitter area, diode) thermionic converter, which is used primarily for other programs at Marquardt. This converter is essentially a scaled-up version of the test cell shown in Figure 7, except that stainless steel is used as the collector material.

3. High-Current Pulse Generator

A high-current pulse generator was designed and fabricated for this program. Silicon controlled rectifiers are used to discharge a variable capacitor bank in a short pulse across the diode, and to provide current for measurements after the pulse discharge. The pulse width and amplitude are continuously variable, as well as the amplitude and rate of decay of current after the pulse is fired. The RC time constant of this circuit can be adjusted to yield an approximately constant output voltage during the current decay process which occurs after the pulse discharge.

C. Experimental Procedure

The experimental procedure for the pulsed discharge experiment can best be illustrated by refering to the typical example shown in Figure 8, which is drawn from photographs of oscilloscope traces obtained during a pulsed discharge and the subsequent current decay. In the initial portion of the trace, before the pulse, the output current is zero, so that the output voltage is equal to the open circuit voltage of 1.3 V. At the beginning of the pulse, the current density increases to 5.3 A per cm^2 as the voltage is increased to 4 V applied. During the pulse the current is approximately constant while the voltage decreases due to the increased ion density and decreased space-charge barrier resulting from electron-atom ionizing collisions. Just after the pulse the current decreases to 2.6 A per cm^2 at an output voltage of 0.5 V. When the circuit is adjusted to maintain the voltage approximately constant an exponential current decay is observed.

Inductive voltage spikes appear on the output voltage trace when the current is changing rapidly. These inductive voltages are not actually present between the emitter and collector, but are due to stray pickup by the wires comprising the voltage probe. This was shown to be the case by a brief experiment in which the electrodes were shorted together and a pulse was applied to the short-circuited converter. Voltage spikes still appeared, which was due to mutual-inductance coupling between the cables supplying the pulse to the diode and the output-voltage probe cables. The inductive voltage was observed to be negligible compared to the output voltage when the current was changing slowly, as during the decay portion of the trace. In later experiments, the inductive reactance was reduced to about 10% of the value

TYPICAL PULSED - DISCHARGE OSCILLOSCOPE TRACES

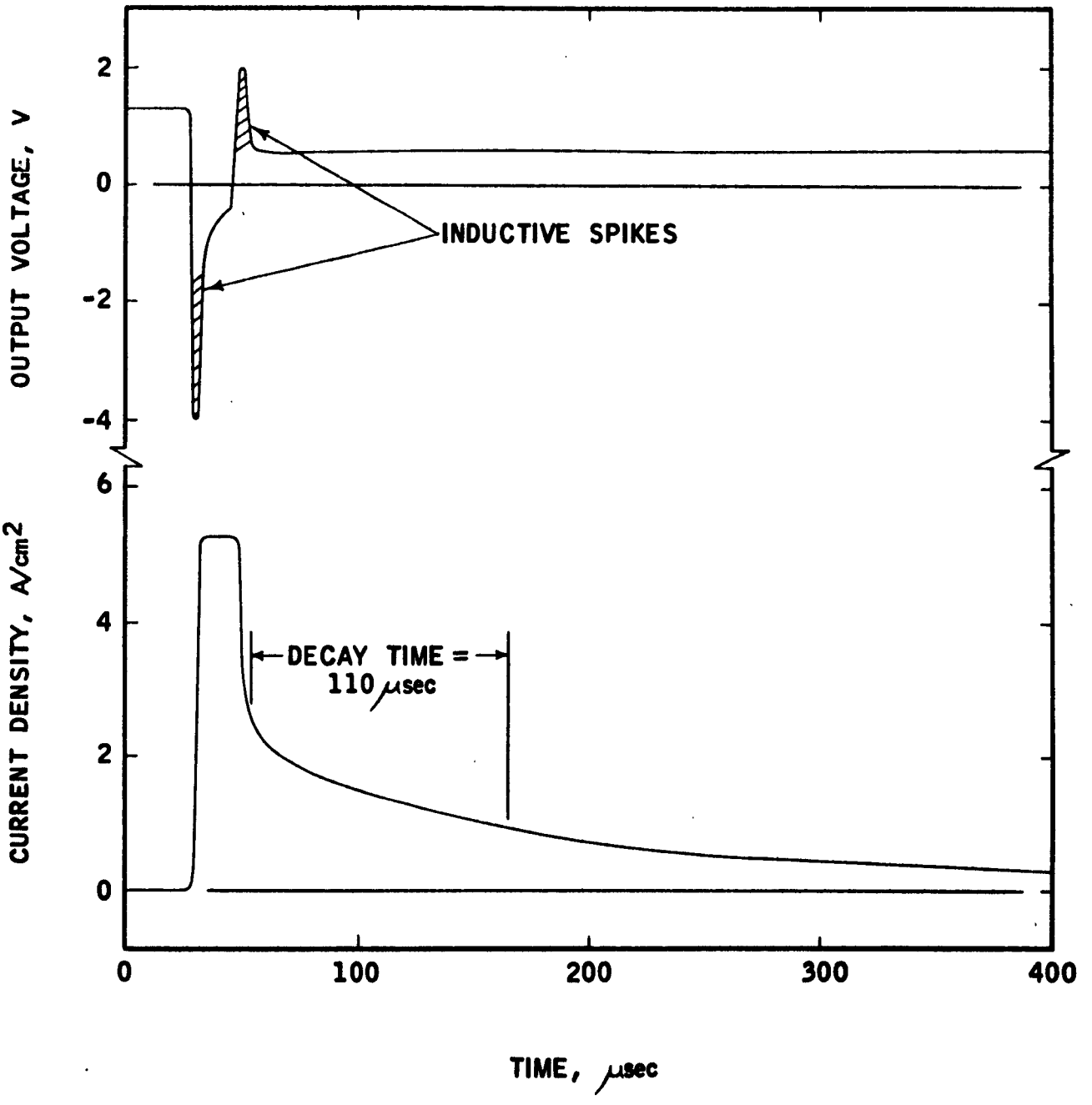

R-14,809

Figure 8

here by using properly designed coaxial voltage and current leads to the diode, and by connecting the current leads so that coaxial current flow is maintained in the diode. (The outer envelope of the diode is used as the return path for the emitter-collector current).

Data reduction consists of measuring the pulse amplitude (maximum voltage and maximum current) and pulse width, as well as the maximum current after the pulse and the time constant of the pulse decay. This time constant is defined as the usual e-folding time τ (the time required for the current density J to decrease to e^{-1} of the initial value J_o just after the pulse) given by

$$J(t) \simeq J_o e^{-\frac{t}{\tau}}$$

$$J(\tau) = J_o/e \ .$$

The steady-state current-voltage characteristics were obtained for comparison with the diode voltage and current just after the pulse. A variable high-current DC power supply was connected across the diode, the output of this supply was varied, and the resultant diode voltage and current were recorded with an x-y recorder. As a check on the characteristics obtained in this manner, the current-voltage characteristic was swept with the output of a 60 cps high-current AC power supply. The characteristic curves were displayed on an x-y oscilloscope and photographed to record the data. The results obtained in this manner agreed fairly well with the DC values.

D. Experimental Results

The results obtained in the pulsed-discharge experiments are summarized in Figures 9, 10 and 11 and are compared to the steady-state current-voltage characteristics at the same operating conditions. Figure 9 shows results obtained with the P1D converter at an emitter temperature of 1300°C and a cesium pressure of 1 torr. Results obtained at 2.7 torr with the P11D converter at emitter temperatures of 1270°C and 1305°C are shown in Figures 10 and 11 respectively.

1. P1D Converter, T_e = 1300°C

Figure 9 compares the steady-state current-voltage characteristic with the current and voltage obtained just after a pulsed discharge. The open-circuit voltage of the steady-state characteristic is 1.6 V. When the output voltage reaches a value of -0.7 V a sudden transition to the ignited-mode branch of the curve is observed. This ignited mode can then be traced in a stable manner provided that the output voltage does not increase beyond about +0.7 V. The maximum power density on the ignited-mode curve is 0.65 W per cm^2, for the indicated cesium pressure of 1 torr. The power density at this emitter temperature can be increased by increasing the cesium pressure, and a further increase can be obtained by reducing the electrode spacing.

COMPARISON OF STEADY-STATE AND PULSED VOLTAGE-CURRENT CHARACTERISTICS

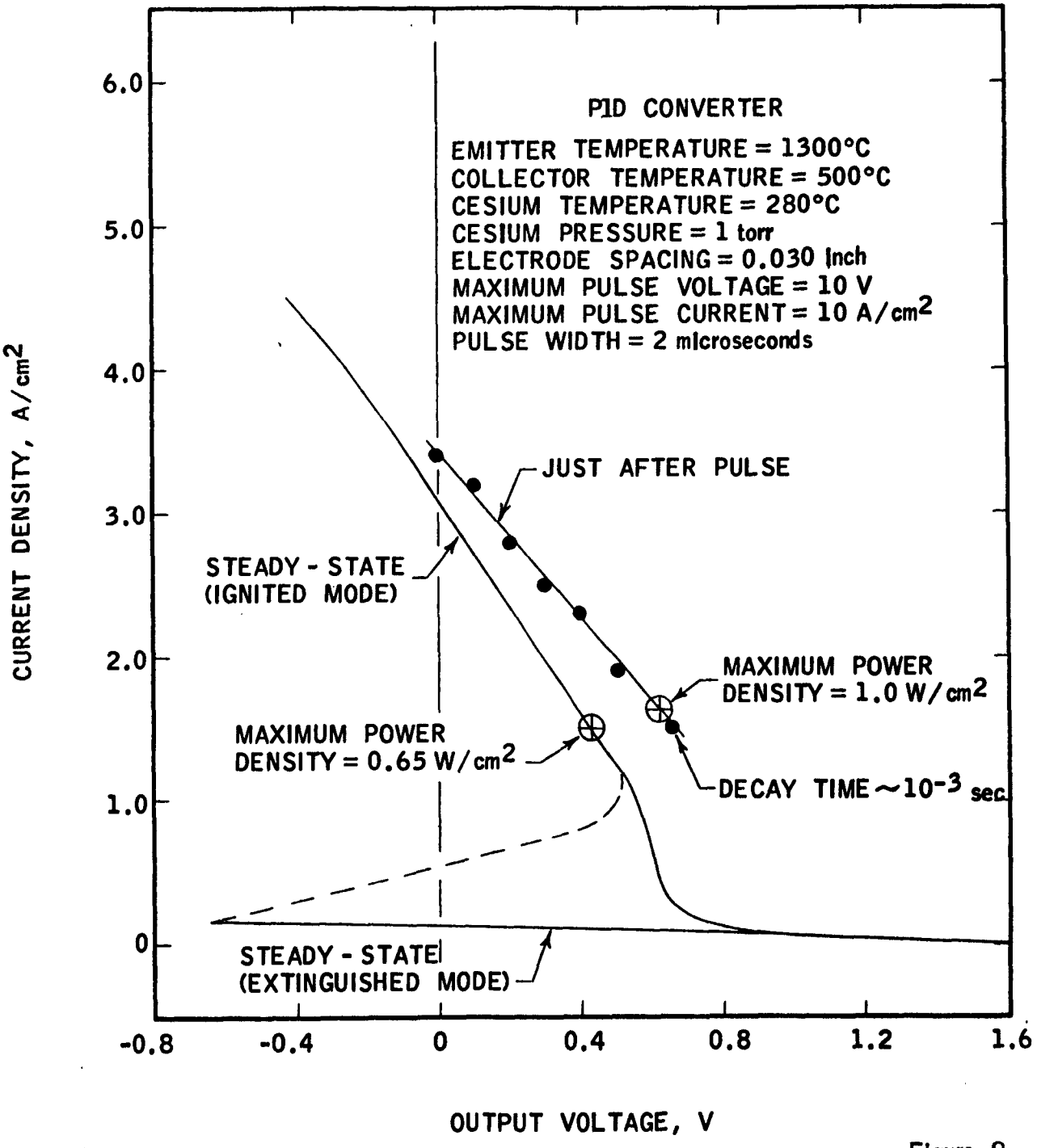

R-14,672

Figure 9

COMPARISON OF STEADY-STATE AND PULSED VOLTAGE-CURRENT CHARACTERISTICS

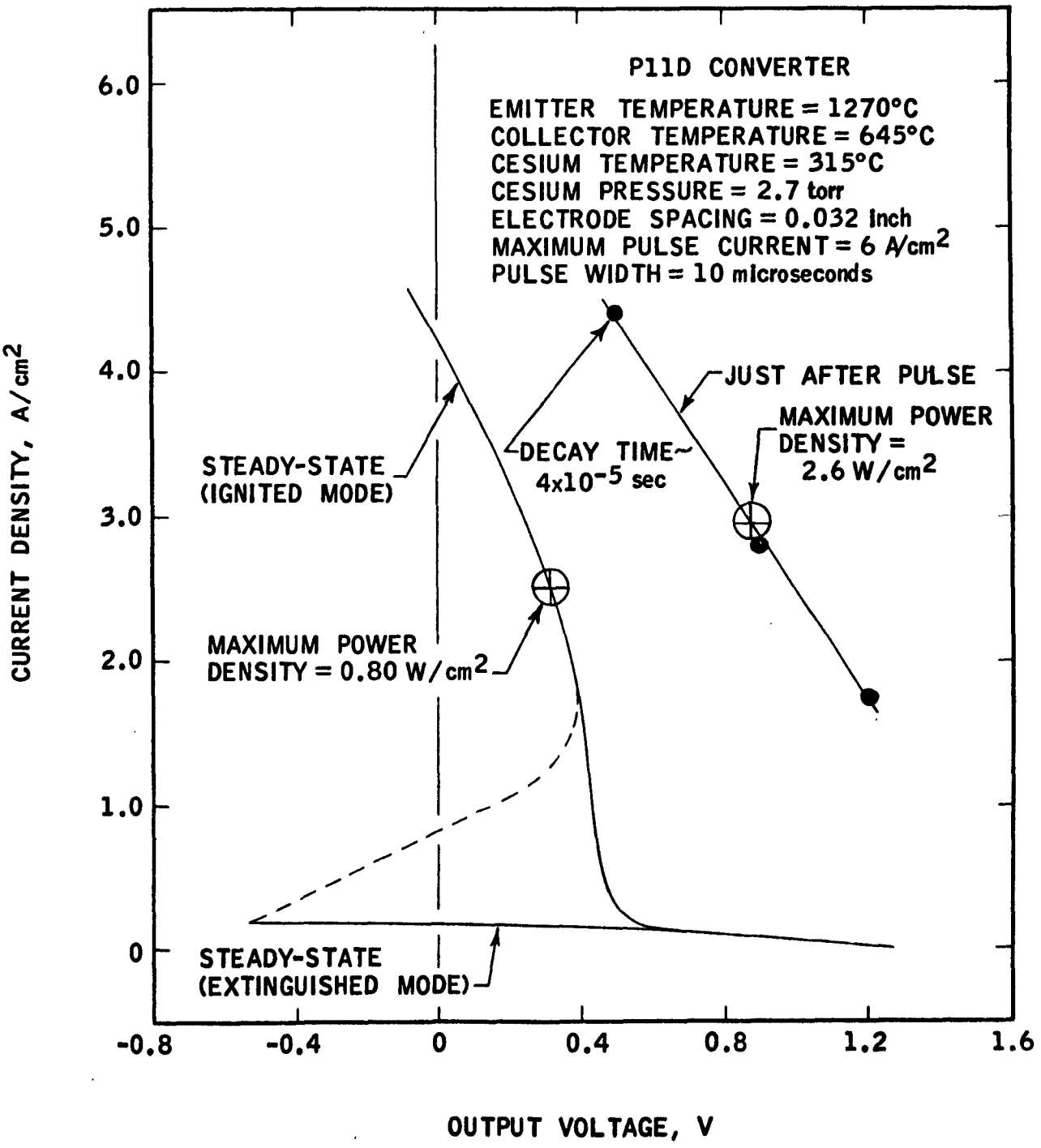

COMPARISON OF STEADY-STATE AND PULSED VOLTAGE-CURRENT CHARACTERISTICS

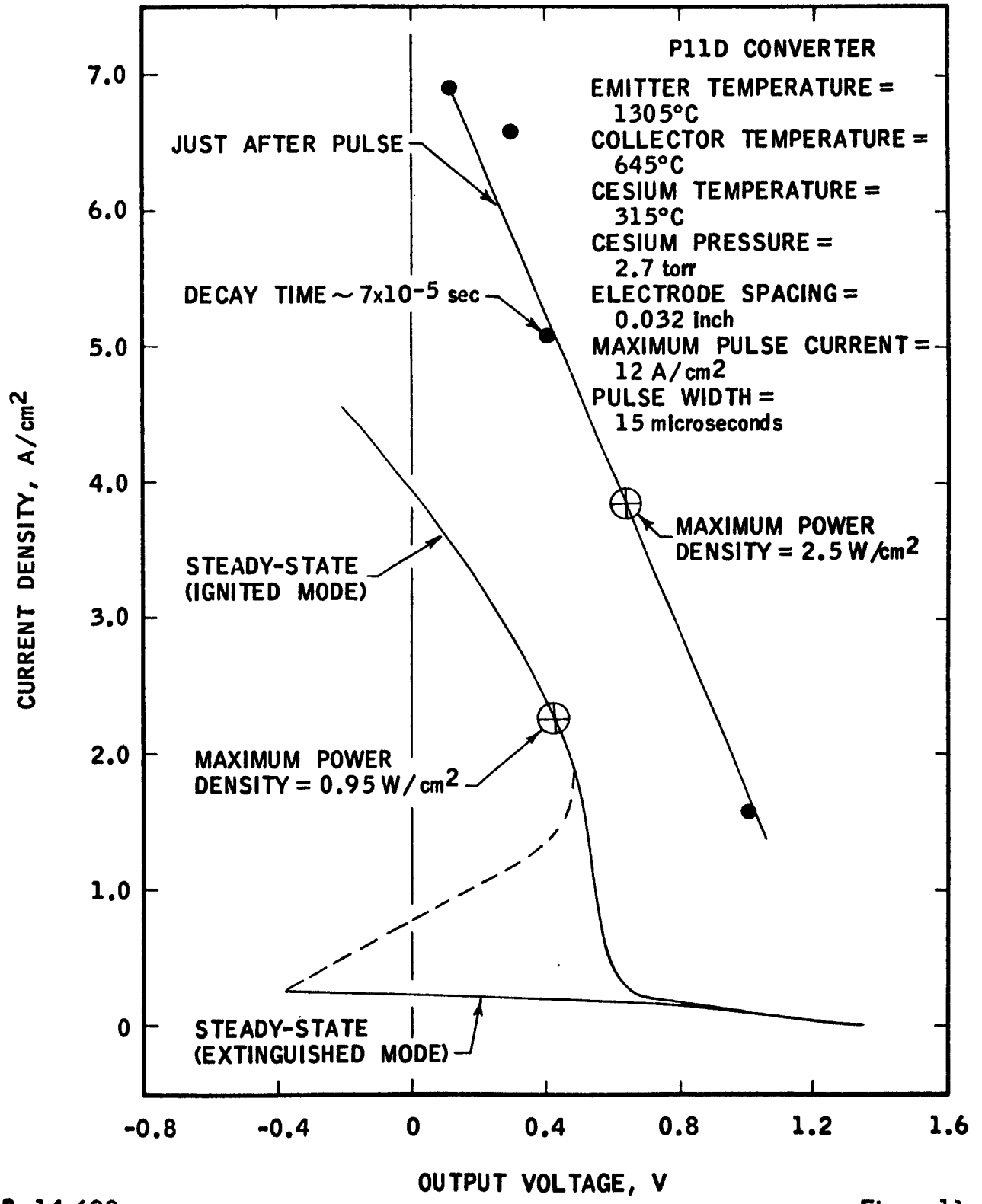

R-14,699

Figure 11

The experimental points corresponding to the voltage and current just after a 10 V, 10 A per cm^2 pulse are shown. The maximum power density for the curve drawn through these points is about 1.0 W per cm^2. At the low-current end of this curve an exponential current decay with a decay time of about 10^{-3} seconds was observed. The decay time corresponding to points at the higher-current end of the curve, near short-circuit conditions, was about 50 to 100 microseconds; this value is only approximate since the voltage was changing during the current decay process due to a mismatch between the time constant of the circuit and the converter. This difficulty was corrected in later experiments.

2. P11D Converter, T_e = 1270°C

The steady-state and pulsed current-voltage characteristics of the P11D converter shown in Figure 10 were obtained at an emitter temperature of 1270°C. The maximum power density for steady-state operation, which occurs on the ignited-mode portion of the characteristic, is 0.80 W per cm^2. *The pulsed characteristics of this converter were obtained with a wider pulse than was used with the P1D converter. At the maximum current on the pulsed characteristic, the decay time was about 40 microseconds; the decay time at higher output voltage and lower current was about two or three times larger than this value. At the maximum power point the output power density is 2.6 W per cm^2.

3. P11D Converter, T_e = 1305°C

The steady-state and pulsed characteristics of the P11D converter were obtained at conditions similar to the preceding experiment except that the emitter temperature was increased to 1305°C. As shown in Figure 11, the results are comparable to those obtained at the lower temperature. The maximum steady-state power density is 0.95 W per cm^2,*whereas the maximum power density on the pulsed characteristic is about 2.5 W per cm^2. The decay time near the center of the pulsed characteristic is 70 microseconds; the decay time near short-circuit conditions is about half of this value, and the decay time at 1 V output voltage is about 100 microseconds.

E. Discussion and Interpretation of Results

The experiments which are summarized in the preceding section should be considered as exploratory measurements to investigate the feasibility of the pulsed-discharge technique for investigating current-limiting factors in thermionic converters. The data indicate that this method can be quite useful in the determination of the basic physical mechanisms that enter into cesium diode operation. These results provide the foundation for a systematic investigation of current-limiting factors and thermionic converter physics.

* This is not the maximum power density for this emitter temperature. The maximum would be obtained by increasing the cesium pressure and decreasing the electrode spacing.

1. Output Current Density

The pulsed current-voltage characteristics in Figure 9 can be compared with the characteristics shown in Figures 10 and 11. Figure 9 was obtained at a cesium pressure of 1 torr, whereas the cesium pressure in Figures 10 and 11 was 2.7 torr. It can be seen that the difference between the pulsed and steady-state curves is much larger at the higher cesium pressure. Of course, the results are not completely comparable since the pulse width and amplitude were different at the different cesium pressures.

It is interesting to compare the current density obtained with the emission-limited current density predicted by electron-emission studies such as those reported by Aamodt, Brown, and Nichols[15]. This reference shows a Langmuir-Taylor diagram for the electron emission of molybdenum in cesium vapor at various pressures. At a surface temperature of 1270°C and a cesium pressure of 2.7 torr, as in Figure 10, this diagram predicts an emission-limited current density of 10 A per cm^2, which corresponds to an effective work function of 2.3 eV. At the high-current end of the pulsed characteristic in Figure 10, the current density is 4.4 A per cm^2 at an output voltage of 0.5 volt. Substitution of this current density into the emission equation

$$J = 120\ T_E^2 \exp\ (-11{,}610\ \phi/T_E)$$

predicts a work function of not more than 2.4 eV, which is in agreement with the Langmuir-Taylor diagram.

This current density is also compatible with the observed output voltage. At the collector temperature used, we would expect a collector work function of about 1.7 eV due to cesium adsorption on the collector surface. The collector Fermi level is displaced with respect to the emitter Fermi level by the output voltage of 0.5 V. Therefore, the space just outside of the collector surface will be at a potential of 0.5 + 1.7 = 2.2 V with respect to the emitter Fermi level. Since the emitter work function is 2.3 to 2.4 eV, we have a net accelerating voltage of 0.1 to 0.2 V across the interelectrode space.

For comparison, we can perform the same type of calculation on the data shown in Figure 9 for a lower cesium pressure. The short-circuit current on the pulsed characteristic in this figure is 3.4 A per cm^2 which corresponds to a work function of 2.5 eV. However, the saturated emission obtained from Reference (15) indicates a current density of 1.5 A per cm^2, corresponding to a work function of 2.6 eV. Two possible causes of this discrepancy are:

1. The saturated emission current indicated by the data in Reference (15) is too low.

2. An excess of positive ions in the interelectrode region gives rise to a strong electric field across a positive sheath near the emitter surface which lowers the emission barrier by 0.1 eV.

The general conclusions that can be drawn from the pulsed-discharge data in Figures 9, 10 and 11 is that the output current at positive values of output voltage can be increased appreciably by increasing the positive ion density. This is particularly true at higher cesium pressures where the pulsed characteristic indicates a much higher current density at each output voltage point than the steady-state characteristic. This is to be expected, since the work function is lowered enough to produce a current density several times larger than would be obtained at 1.0 torr.

2. Interelectrode Potential and Positive Ion Mobility

The current decay times measured in these experiments allow an estimate to be made of the potential in the interelectrode region. This estimate is based on the hypothesis that the transit time for positive ions from the interelectrode space to the emitter and/or collector electrodes is approximately equal to the observed decay time. This seems reasonable since the increase in current over the steady-state value depends upon the increased ion density supplied by the pulsed discharge.

As indicated in Appendix A, the primary collision process contributing to the ion mobility is charge-exchange collisions, which impede the motion of positive charge to the electrodes. To determine whether charge exchange is important under our experimental conditions, the mean free path for a charge-exchange collision will be compared with the emitter-collector spacing.

The mean free path for ion-atom collisions is given in terms of the average atomic cross section $\bar{Q}$ and the average atom density $\bar{N}$ as

$$\lambda = \frac{1}{\bar{N}\,\bar{Q}} .$$

As indicated in Appendix A, charge exchange will be the dominant collision process, with $\bar{Q} \approx 2 \times 10^{-13}$ cm^2. The average gas temperature is assumed to be equal to the average of the emitter and collector temperatures, yielding $T_g = 1250°K$. The cesium pressure is 2.7 torr, so that the gas density is

$$\bar{N} = 9.67 \times 10^{18} \frac{p}{T_g} = 2.1 \times 10^{16} \text{ atom/cm}^3 .$$

This yields a mean free path of 2.4×10^{-4} cm. Since the emitter-collector spacing of 8.1×10^{-2} cm is much larger than the mean free path, an ion will be scattered many times before reaching the emitter or collector surface, and the mobility equation can be used to examine the ion motion.

The ion mobility is

$$\mu = \frac{3.06\sqrt{T_g}}{p} \quad \text{cm}^2/\text{V-sec}$$

which yields $\mu = 40$ cm^2/V-sec. The mobility equation,

$$V = \mu E,$$

can be written as

$$\Delta V = \frac{(\Delta X)^2}{\mu \Delta t}$$

where ΔX is the distance an ion travels in a time Δt, and the electric field is $E = \Delta V/\Delta X$.

This equation can be applied to the pulsed discharge experiment by approximating the (unknown) potential distribution during the decay process after the pulse by a linear one. There is an excess of positive charge in the interelectrode region, so that the electric field will drive ions to the emitter and/or collector surfaces, where recombination occurs. ΔV is the potential V at the middle of the interelectrode gap minus the potential just outside of the emitter or collector. Δt is the decay time, t, and ΔX is w/2, one half of the spacing, so that

$$V = \frac{w^2}{4\mu t} .$$

Figure 11 indicates a decay time of 7×10^{-5} second, so that the voltage calculated in this manner is V = 0.6 volt.

At this point it is interesting to consider the implications of this calculated voltage of 0.6 V. The ion energy corresponding to this voltage is considerably larger than the expected thermal energy of positive ions, given by

$$\frac{3}{2}\frac{kT_g}{e} \approx 0.15 \text{ V}.$$

Therefore, the magnitude of the decay times observed will require the presence of a voltage gradient if the mobility considerations in Appendix A are valid. This voltage would be maintained by a slight excess of positive ions over electrons in the interelectrode region. The positive ions would be supplied by ionizing collisions of electrons accelerated into the positive region[16].

A recent qualitative calculation[17] indicates that electron emission from the emitter of a thermionic converter may still be space-charge limited even though part of the interelectrode volume is at a positive potential. This physical picture requires an "S" shaped potential distribution such that the interelectrode region is negative (with respect to the top of the emitter work-function barrier) near the emitter and positive near the collector. The calculation referred to does not consider the effect of a finite ion mobility, which will certainly modify the potential distribution.

The exploratory measurements reported here, together with the calculations summarized in Appendix A, indicate that ion mobility due to charge-exchange collisions may play an extremely important part in determining the current-limiting factors in cesium thermionic converters. Further quantitative work is required to obtain a better understanding of the importance of these factors. It seems reasonable to expect that this improved understanding will show the way toward increasing the output current and improving the performance of the intermediate-temperature thermionic converter.

VI. FUTURE APPROACH

A. Pulsed Measurements of Current Density

Future measurements are planned to extend the measurements of the current decay after a pulse. The extension of work will include measurements over a wider range of parameters and observation of characteristics which were not previously studied. The increased range of parameters to be studied should assist in separating the volume and surface ionization effects by providing a range of data where one or the other of these effects predominates.

Information relative to the physical process controlling the production and loss of cesium ions in the interelectrode region will also be obtained from the pulse decay measurements. For example, a short decay time implies that the interelectrode region is at a positive potential with respect to the emitter. Under these conditions, electrons will be accelerated across a sheath away from the emitter surface, and may be capable of ionizing cesium atoms in the interelectrode volume.

B. Investigation of Volume Ionization Ignition

An "ignition" transition associated with volume ionization is often observed during cesium diode operation. This is indicated by either a discontinuous voltage-current characteristic curve, or by a discontinuous change in the slope of the curve. These transitions are observed to occur in the lower-temperature and intermediate-temperature thermionic converters. The ignition process is accompanied by increased power output caused by the ensuing high current level.

In these studies ignition will be achieved by rapidly switching a charged capacitor across the diode output and observing the voltage level at which the transition occurs. The various criteria for obtaining ignition will be noted. The time delay between switching the capacitor across the diode and ignition will be recorded as a function of the capacitor voltage and charge transferred through the diode. It is expected that a higher capacitor voltage will result in a faster transition to volume ionization. Observation of the transient current during the ignition process will yield data on the total charge before ignition takes place as a function of the ignition voltage and the diode parameters.

It is expected that data obtained in these experiments will aid in identifying the ionization mechanism when ignition occurs. Information concerning stability of the volume-ionization mode of operation will be obtained.

C. Analysis of the Relationship Between Surface and Volume Effects

The investigation of current-limiting factors involved in the operation of a thermionic converter may be considered to be a study of two basic mechanisms: 1) the electron producing process (a surface effect) and 2) the process through which the space charge is modified by the introduction of positive ions (surface and volume ionization effects). The mechanisms involved cannot be treated separately in a study of thermionic converters. The operation of a converter depends upon a complex relationship between volume and surface conditions. Some research which has been done, attempts to discover relationships between the converter environment parameters and performance characteristics of the converter. However, part of the difficulty in interpreting some of the published experimental results is caused by inadequate experimental control over the different mechanisms involved in the effect under investigation. Thus, effects are not well-separated for analysis and reliable conclusions cannot be arrived at.

It is expected that the data obtained in this program will provide verification and possibly numerical constants for some of the theories in the literature that pertain to volume and surface effects in cesium diode operation. In some cases the data will be used for correction of existing theories or possibly as a basis for the formation of new theories. It is expected that this increased understanding of the basic mechanisms of cesium diode operation will provide a basis for improving operation of the intermediate-temperature thermionic converter.

APPENDIX A

CHARGE EXCHANGE COLLISIONS AND ION MOBILITY IN CESIUM THERMIONIC CONVERTERS

1. Importance of Charge Exchange in Cesium Diode Thermionic Converters

In the cesium diode thermionic converter, positive cesium ions are required for the neutralization of electron space charge. Positive ions are produced by either surface or volume ionization, or sometimes both. Charge exchange collisions are important because they can reduce the velocity of positive ions within or across the interelectrode space.

When charge exchange occurs between a positive ion and a neutral atom, an electron is transferred from the atom to the ion, so that the ion is neutralized and the initially-neutral atom becomes a positive ion. If the ions are moving with a directed velocity due to either an electric field or a density gradient, charge exchange collisions tend to randomize the transport velocity of positive charge. (This will be explored in more detail in the next section).

Charge exchange is particularly important in the high-cesium-pressure thermionic converter operating in the ignited mode. For this mode of operation positive ions are produced by volume ionization in the interelectrode cesium gas[16]. Slowing down the positive ion motion to the electrodes, where surface recombination occurs, results in an increased ion density in the interelectrode volume. This will drive the interelectrode space more positive, which in turn can result in an increased volume ionization rate if the ionization is due to electron acceleration and subsequent ionizing collisions. Equilibrium will be reached when the ion loss rate due to the increased electric field equals the increased ion production rate.

Charge exchange between ions and neutrals of the same species is a resonant reaction (large cross-section) since the total energy of the (ion plus atom) system will not change appreciably. That is, the energy required for the process

$$Cs_A^+ + Cs_B \longrightarrow Cs_A + Cs_B^+$$

is very small or zero due to symmetry. If the kinetic energy difference between the ion and the atom before collision is small, then the charge exchange cross-section will be much larger than the elastic scattering cross section. This is not the case for a charge exchange collision between different species, since the difference in ionization potentials requires kinetic energy to be liberated or absorbed. For example, the cross-section for the process

$$Ar + Ne^{+} \longrightarrow Ar^{+} + Ne + \text{Kinetic Energy}$$

is smaller than the elastic scattering cross-section.

2. How Charge Exchange Reduces the Charge Transport Velocity

The method by which charge exchange reduces the charge transport velocity will be illustrated by first considering a simplified case in which the ion A^+ is moving parallel to an electric field and the neutral atom B is stationary. Charge exchange is a quantum-mechanical process; however, a classical description of the mass motion of the two particles is an extremely good approximation. It is convenient to consider the impact parameter b for a charge exchange collision:

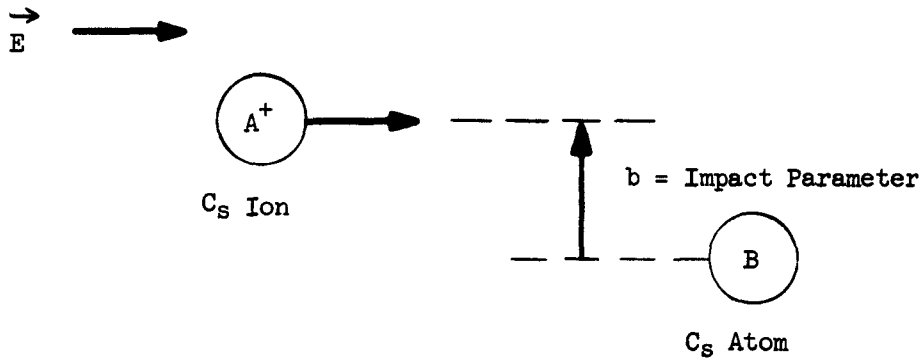

There is a critical value, b_c, of the impact parameter, such that the possibility of charge exchange is 1/2 at $b = b_c$.[18] For $0 \leqslant b < b_c$, the probability of charge exchange oscillates between 0 and 1 with an average value of 1/2, and for b slightly larger than b_c the probability is essentially zero (i.e., for $b > b_c$, the probability goes rapidly to zero with increasing b; $P \sim e^{-\alpha b}$ where $\alpha b_c \gg 1$).

In Figure 12 the motion is approximated by classical hard-elastic-sphere scattering, with the ion (atom) diameter equal to b_c. Charge exchange is an elastic collision process in the sense that the total kinetic energy and the linear momentum are both conserved. This scattering process is illustrated for several different collision-plane angles. Case 1 in Figure 12 shows a head-on collision between the ion A^+ and the atom B. After the collision, A is motionless and B^+ is carrying the charge with no change in direction or velocity, so that the collision has no effect upon charge transfer. In Case 2, a scattering collision is shown for a 45° angle between the collision plane and the initial velocity of A^+. After the collision, B^+ has a velocity component in the direction of the electric field which is one-half of the original charge velocity. Case 3 shows the worst possible case for charge transport, which is a glancing collision that leaves the positive charge with zero velocity just after the collision.

CHARGE EXCHANGE COLLISIONS

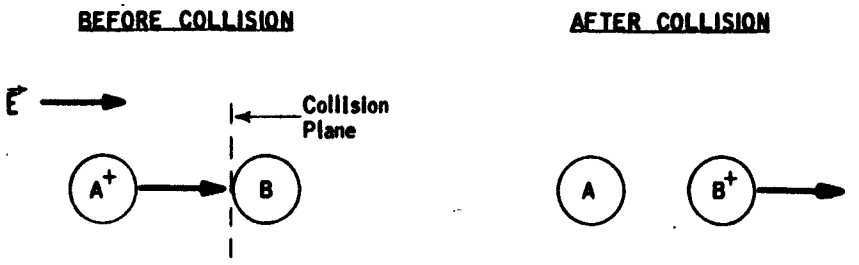

1 - COLLISION PLANE AT 90°

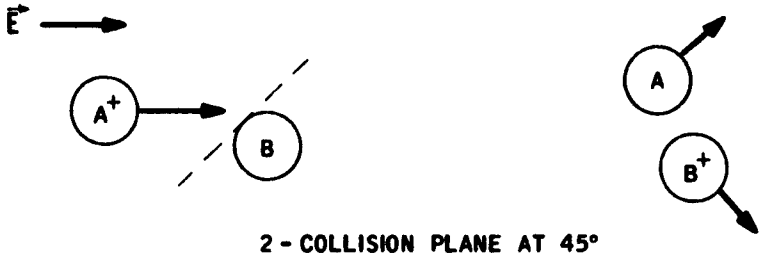

2 - COLLISION PLANE AT 45°

3 - COLLISION PLANE AT 0°

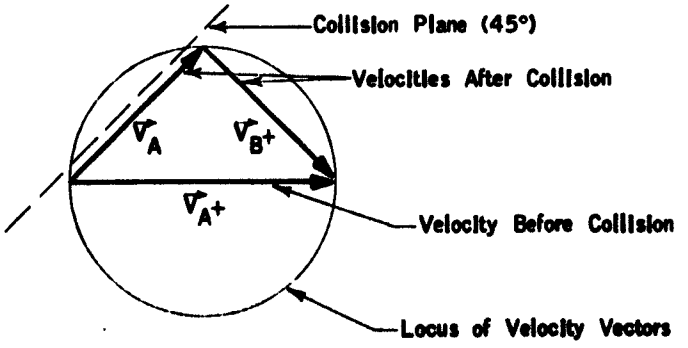

R-14,896

Figure 12

Conservation of kinetic energy and momentum result in the vector diagram shown at the bottom of Figure 12. If the initial velocity of the ion is drawn as the diameter of a circle, then the circle is the locus of all possible velocity vectors after the collision. It can be seen that the component of the charge velocity in the direction of the electric field varies from zero to V_{A^+}, the initial charge velocity, so that, on the average, charge transport will be slowed down by charge exchange collisions.

If the atom B is moving due to thermal energy, then charge exchange collisions with B moving toward A^+ are more probable than collisions with B moving away from A^+. Therefore, increasing gas temperature will result in increased slowing down of charge transport, as compared to the simplified case discussed above.

This simple picture is complicated by polarization forces, since an ion induces dipole moments on neighboring atoms and interacts with the resultant dipoles. The attraction due to polarization increases the effective charge exchange cross-section. In cesium this dipole interaction becomes important when the ion energy is 1 eV or less.

3. Momentum Exchange Cross Section for Charge Exchange Collisions

In a recent calculation[19], J. W. Sheldon has calculated the charge exchange cross section by extrapolating experimental cross-section data to low ion energies. His extrapolation formula is based on the theoretical form of the charge exchange cross section, and a correction for polarization effects is included. The experimental data cover the ion energy range from 6 to 10,000 eV, whereas in a cesium diode an energy range of about 0.1 to 1 eV is of interest. Since the extrapolation is over a comparatively small energy difference, Sheldon's calculations should be reasonably accurate. Sheldon used four different sets of experimental data[20-23]. The momentum exchange cross section Q (twice the collision cross section) calculated for an ion-atom relative energy of 0.1 eV varies from about 1.3×10^{-13} to 3.0×10^{-13} cm^2.

4. Positive Ion Mobility

To describe the average ion motion with an applied electric field, the mobility equation is used. The mobility is defined as a ratio of the equilibrium ion velocity (the velocity after many collisions) to the electric field, so that

$$\vec{v} = \mu \vec{E}.$$

The mobility is calculated from the average momentum exchange cross-section $\bar{Q}$ as[18]

$$\mu_o = \frac{3\sqrt{\pi}}{8} \frac{e}{N_o \bar{Q}} \frac{1}{\sqrt{M\, k\, T_g}}$$

where M is the mass of the atom (ion), k is Boltzmann's constant, T_g is the gas temperature, N_o is the standard gas density (2.69×10^{19} atom per cm^3) at 0°C and 760 torr.

An equation of this form (in error by a numerical constant) can be derived by making some simplifying assumptions. The random velocities of the cesium ions and atoms will be assumed equal (ions in thermal equilibrium with gas), and the average directed velocity of the ion just after a collision will be assumed to be zero (complete randomization after a collision).

The average time interval $\bar{t}$ between collisions is given by

$$\bar{t} = \frac{\lambda}{\bar{c}}$$

where λ is the ionic mean free path and $\bar{c}$ is the mean velocity of the ion, given by kinetic theory as

$$\tfrac{1}{2} M\bar{c}^2 = \frac{4 k T_g}{\pi}$$

$$\bar{c} = \sqrt{\frac{8 k T_g}{M}} ,$$

so that

$$\bar{t} = \lambda \sqrt{\frac{\pi M}{8 k T_g}} .$$

On the average, the ion is accelerated between collisions from zero velocity to a maximum velocity given by

$$\vec{v}_{max} = \vec{a}\,\bar{t} = \frac{e\vec{E}}{M}\bar{t} .$$

The average velocity (drift velocity) is one half of the maximum velocity,

$$\vec{v}_{av} = \frac{e\vec{E}}{2M}\bar{t} = \frac{e\lambda}{2M}\sqrt{\frac{\pi M}{8 k T_g}}\,\vec{E} ,$$

so that the mobility is

$$\mu = \frac{e\lambda}{2}\sqrt{\frac{\pi}{8 M k T_g}} .$$

In terms of the momentum exchange cross section $\bar{Q}$, given by

$$\lambda = \frac{1}{N\bar{Q}}$$

the mobility is

$$\mu = \left(\frac{1}{2}\sqrt{\frac{\pi}{8}}\right)\frac{e}{N\bar{Q}}\,\frac{1}{\sqrt{M k T_g}}$$

$$\mu = 0.313\,\frac{e}{N\bar{Q}}\,\frac{1}{\sqrt{M k T_g}} .$$

There are two criticisms of this simplified derivation. 1) The probability for forward scattering is greater than that for backward scattering, so that the average directed velocity $\overline{V_o}$ just after collision is not zero. 2) The average time $\overline{t}$ between collisions depends upon the direction of scattering.

A rigorous derivation of the mobility, which takes into account the statistical distributions of $\overline{t}$ and $\overline{V_o}$, yields[24]

$$\mu = \frac{3\sqrt{\pi}}{8} \frac{e}{N\bar{Q}} \frac{1}{\sqrt{M\,k\,T_g}} ,$$

$$\mu = 0.666 \frac{e}{N\bar{Q}} \frac{1}{\sqrt{M\,k\,T_g}} .$$

It can be seen that this differs from the expression derived here by about a factor of 2.

The average momentum-exchange cross section $\bar{Q}$ is obtained by integrating over the Boltzmann distribution about the gas temperature under consideration. Sheldon has performed this calculation[19], which yields $\bar{Q} = 2 \times 10^{-13}$ cm^2 for a gas temperature of 300°K. The corresponding mobility* is $\mu_o = 0.0632$ cm^2/(V-sec).

To apply this equation to the cesium diode, we will assume that $\bar{Q} = 2 \times 10^{-13}$ cm^2 and is independent of the gas temperature. Figure 1 in Sheldon's calculation indicates that the cross section will not change drastically over the gas temperature range considered here.

The above mobility, $\mu_o = 0.0632$ cm^2/V-sec at $T_G = 300$°K, has been reduced to the standard gas density of $N_o = 2.69 \times 10^{19}$ atom per cm^3. This gas density corresponds to $p_o = 760$ torr and $T_o = 273$°K. To find the mobility at a different gas density, it can be noted that

$$N = N_o \frac{p}{p_o} \frac{T_o}{T_g} ,$$

* Sheldon has calculated four values of mobility from the four sets of experimental reference data used[20-23]. The value given here is the average of Sheldon's four values. $\bar{Q}$ is calculated from this average mobility.

so that

$$\mu = \mu_o \frac{p_o}{p} \frac{T_g}{T_o} .$$

If the gas temperature under the square root sign (the gas-kinetic term) in the expression for the mobility is also allowed to change, then

$$\mu = \mu_o \left(\frac{760}{p}\right)\left(\frac{T}{273}\right)\sqrt{\frac{300}{T}} .$$

Using Sheldon's value of μ_o = 0.0632 $cm^2/(V\text{-}sec)$,

$$\mu = \frac{3.06\sqrt{T_g}}{p} ,$$

where T_g is in °K

p is in torr.

This is the formula for the mobility used in this report.

REFERENCES

1. J. Kaye & J. A. Welsh, "Direct Conversion of Heat to Electricity", Wiley & Sons, N. Y., 1960.

2. R. A. Laubenstein, W. Beyermann, C. Kaplan & W. Wise:
   a) Marquardt Report No. 25,039, February 1962
   b) Marquardt Report No. 25,075, February 1963

3. H. L. Garvin, W. B. Teutsh & R. W. Pidd, J. Appl. Phys. 31, 1508 (1960).

4. R. J. Zollweg & M. Gottlieb, J. Appl. Phys. 32, 890 (1961).

5. J. M. Houston, "Oscillations in Cesium Thermionic Converters" Report on Twenty-Second Annual Conf. on Physical Electronics, M.I.T., March 1962.

6. N. D'Angelo, Phys. Fluids 4, 1054 (1961).

7. P. L. Auer, J. Appl. Phys. 32, 2611 (1961).

8. A. L. Eichenbaum & K. G. Hernqvist, J. Appl. Phys. 32, 16 (1961).

9. K. P. Luke & F. E. Jamerson, J. Appl. Phys. 32, 321 (1961).

10. E. N. Carabateas & M. F. Koskinen, "Oscillations Observed in Cesium Thermionic Converters", Proceedings of the Third Government-Industry Thermionic Roundtable Discussions, Vol. I, 1961.

11. P. J. Shaver, Proc. of Twenty-Second Annual Conf. on Physical Electronics, M.I.T., March 1962.

12. J. F. Waymouth, Sylvania Technologist 13, 2 (1960).

13. G. A. Hass, N.R.L. Report 5657, U. S. Naval Research Laboratory, October 1961.

14. C. Kaplan, Report on Twenty-Second Annual Conf. on Physical Electronics, M.I.T., March 1962.

15. R. L. Aamodt, L. J. Brown, and B. D. Nichols, J. Appl. Phys. 33, 2080 (1962).

16. W. B. Nottingham, Tech. Report No. TEE-7002-5, Thermo Electron Engineering Corp., Waltham, Mass., September 1960.

17. S. S. Kitrilakis, M. E. Meeker, & N. S. Rasor Contract Nonr 3563(00), Report No. 2-63, Thermo Electron Engineering Corp., Waltham, Mass., 1962.

18. T. Holstein, J. Phys. Chem. 56, 832 (1952).

19. J. W. Sheldon, J. Appl. Phys. 34, 444 (1963).

20. R. M. Kushnir, B. M. Palyukh, and L. A. Sena, Bull. Acad. Sci. USSR, Phys. Ser (English Transl.) 23, 995 (1959).

21. A. M. Bukhteev and Yu. F. Bydin, Bull. Acad. Sci. USSR, Phys. Ser (English Transl.) 24, 966 (1960).

22. R. M. Kushnir and I. M. Buchma, Bull. Acad. Sci. USSR, Phys. Ser (English Transl.) 24, 989 (1960).

23. R. C. Speiser, EOS Report 1583, Electro-Optical Systems, Inc., Pasadena, California (1961).

24. N. F. Mott & H. S. W. Massey, "The Theory of Atomic Collisions", Chapter XII, Second Edition, Oxford, 1949.

March 1963 Report 25,081

DISTRIBUTION LIST

	No. Copies
Office of Naval Research Power Branch (Code 429) Department of the Navy Washington 25, D. C.	4
Cognizant ONR Area Branch Office Dr. Wesley Rigg Office of Naval Research 1030 E. Green Street Pasadena, California	1
U. S. Naval Research Laboratory Technical Information Division Washington 25, D. C.	6
Commanding Officer Office of Naval Research Branch Office Box 39 Navy #100 Fleet Post Office New York, New York	2
Office of Technical Services Department of Commerce Washington 25, D. C.	1
Armed Services Technical Information Agency Arlington Hall Station Arlington 12, Virginia	10
National Aeronautics & Space Administration 1520 H. Street, N. W. Washington 25, D. C. Attn: James J. Lynch	1
National Aeronautics & Space Administration Lewis Research Center 21000 Brookpark Road Cleveland 35, Ohio	
Attn: H. Schwartz	1
Roland Breitweiser	1
Bernard Lubarsky	1
William LaGray	1
R. P. Migra	1
Chief of Naval Operations (OP-07G) Department of the Navy Washington 25, D. C.	1

DISTRIBUTION LIST - Cont'd

Commandant, U. S. Marine Corps
Code CSY-3
Headquarters, Marine Corps
Washington 25, D. C. 1

Chief, Bureau of Ships
Department of the Navy
Washington 25, D. C.
Attn: Code 342B 2
Code 1500 Mr. Wm. Hewitt 1
Code 456B, Mr. V. Gardner 1
Code 210L 2

U. S. Atomic Energy Commission
Division of Reactor Development
Washington 25, D. C.
Attn: SNAP Reactor Branch 1
Direct Conversion Branch 1
Army Reactor & Water Systems Branch 1
Isotope Power Branch 1

U. S. Atomic Energy Commission
San Francisco Operation Office
2111 Bancroft Way
Berkeley 4, California
Attn: Reactor Division 1

Aeronautical Systems Division
ASRMFP-2
Wright Patterson Air Force Base
Ohio 1

Air Force Cambridge Research Center
(CRZAP)
L. G. Hanscom Field
Bedford, Massachusetts 1

Power Information Center
University of Pennsylvania
Moore School Building
200 South 33rd Street
Philadelphia 4, Pennsylvania 1

Director of Special Projects (SP-001)
Department of the Navy
Washington 25, D. C. 10

DISTRIBUTION LIST - Cont'd

Los Alamos Scientific Laboratory
Post Office Box 1663
Los Alamos, New Mexico
Attn: Dr. George M. Grover 1

Argonne National Laboratory
9700 South Cass Avenue
Argonne, Illinois
Attn: Aaron J. Ulrich 1

Director, Advanced Research Projects Agency
The Pentagon
Washington 25, D. C.
Attn: Dr. John Huth 1

U. S. Army Electronic R&D Laboratory
Fort Monmouth, New Jersey
Attn: Dr. Emil Kittl 1

Mr. A. F. Underwood
Manager, General Motors Research Labs.
12 Mile and Mound Road
Warren, Michigan
Attn: Dr. F. Jamerson 1

Atomics International
Post Office Box 309
Canoga Park, California
Attn: Dr. R. C. Allen 1

General Atomic
Post Office Box 608
San Diego 12, California
Attn: Dr. R. W. Pidd 1

ARACON Laboratories
Virginia Road
Concord, Massachusetts
Attn: Dr. S. Ruby 1

Ford Instrument Company
3110 Thomson Avenue
Long Island City, New York
Attn: T. Jarvis 1

Armour Research Foundation
10 W. 35th Street
Chicago 16, Illinois
Attn: Dr. D. W. Levinson 1

DISTRIBUTION LIST - Cont'd

Jet Propulsion Laboratory
California Institute of Technology
4800 Oak Grove Drive
Pasadena, California
Attn: P. Rouklove 1

RCA Laboratories
David Sarnoff Research Center
Princeton, New Jersey
Attn: Dr. Paul Rappaport 1

The Martin Corporation
Baltimore 3, Maryland
Attn: Dr. M. Talaat 1

Thermo Electron Engineering Corporation
85 First Avenue
Waltham 54, Massachusetts
Attn: Dr. George Hatsopoulos 1

Hughes Research Laboratories
3011 Malibu Canyon Road
Malibu, California
Attn: Dr. R. C. Knechtli 1

Thompson Ramo Wooldridge, Inc.
7209 Platt Avenue
Cleveland 4, Ohio
Attn: Wm. J. Leovic 1

General Electric Research Laboratory
Schenectady, New York
Attn: Dr. V. C. Wilson 1

The Marquardt Corporation
ASTRO
16555 Saticoy Street
Van Nuys, California
Attn: Dr. R. Laubenstein 1

Texas Instruments, Inc.
Post Office Box 5474
Dallas 22, Texas
Attn: Dr. R. A. Chapman 1

University of Denver
Colorado Seminary
Denver Research Institute
Denver 10, Colorado
Attn: Dr. Charles B. Magee 1

DISTRIBUTION LIST - Cont'd

Radio Corp. of America
Electron Tube Division
Lancaster, Pennsylvania
Attn: F. G. Block 1

Electro Optical Systems Inc.
300 N. Halstead Ave.
Pasadena, California
Attn: Dr. A. O. Jensen 1

General Electric Company
Post Office Box 846
Atomic Product Division
Vallecitos Laboratory
Pleasenton, California
Attn: Robert Scott 1

General Electric Company
Power Tube Division
1 River Road
Schenectady 5, New York
Attn: Mr. D..L. Schaefer 1

Consolidated Controls Corporation
Bethel, Connecticut
Attn: Mr. David Mends 1

Institute for Defense Analysis
1666 Connecticut Avenue, N. W.
Washington, D. C.
Attn: Mr. Robert Hamilton 1

Research Laboratories Library
General Motors Corporation
General Motors Technical Center
P. O. Box 388
Warren, Michigan
Attn: Dr. F. Jamerson 1

Knolls Atomic Power Laboratory
Schenectady, New York
Attn: Dr. R. Ehrlick 1

AD

Marquardt Corp., Van Nuys, Calif.
INVESTIGATION OF THE CURRENT DENSITY LIMITATIONS IN A THERMIONIC CONVERTER by C. Kaplan, Annual Summary Report for 1 March 62 - 28 Feb. 63, 44p. incl. illus., 24 refs.
(Contract Nonr 3738(00))

Unclassified Report

Oscillations in grid voltage, output voltage and output current were observed over a wide range of operating conditions with a cesium-vapor triode. At higher cesium pressures, the oscillation period is an increasing function of the cesium pressure, which implies that the oscillations are controlled by scattering of positive ions in the interelectrode region. An approximate calculation of the ion accelerating voltage required to transfer ions from the middle of the emitter-collector space to the collector indicates a voltage of between 0.5 and 1.0 volt. This calculation is based on collisionless ion transport at low cesium pressures and ion transport dominated by charge-exchange collisions at high cesium pressures. It was observed that the oscillations stop at a definite point on the current-voltage characteristic.

Pulsed-discharge experiments were initiated to investigate current-density limiting factors in a cesium diode operating in the intermediate temperature range. The experimental technique consisted of applying a pulsed discharge to the test cell and observing the effect upon output current after the pulse. When the diode operation was space-charge limited, a large increase in current was observed after the pulse; whereas if the current was nearly emission limited, only a small increase was observed. Reasonable agreement was obtained between the current density measured after a pulsed discharge and the saturated electron current density obtained from the literature. Measurements of the time required to establish equilibrium after the pulsed discharge providnd information on the physics of cesium diode thermionic converters. A calculation based upon the experimental measurements indicates that charge-exchange collisions will control ion transport to the emitter or collector, where surface recombination will occur.

(over)

UNCLASSIFIED

I. Thermionic energy conversion
II. Kaplan, C.
III. Office of Naval Research
IV. Contract Nonr 3738(00)

UNCLASSIFIED

Calculations have been performed based upon a literature survey of charge exchange collisions and ion mobility in cesium vapor. Charge exchange collisions result in a slowing down of positive-charge transfer within or across the interelectrode volume. The exploratory measurements of this report, together with the calculations summarized in Appendix A, indicate that charge exchange collisions may play an important part in determining the current-limiting factors in cesium thermionic converters.

UNCLASSIFIED

UNITERMS
Thermionics
Energy
Ions
Arc
Electric

UNCLASSIFIED

AD

Marquardt Corp., Van Nuys, Calif.
INVESTIGATION OF THE CURRENT DENSITY LIMITATIONS IN A THERMIONIC CONVERTER by C. Kaplan, Annual Summary Report for 1 March 62 - 28 Feb. 63, 44p. incl. illus., 24 refs.
(Contract Nonr 3738(00))

Unclassified Report

Oscillations in grid voltage, output voltage and output current were observed over a wide range of operating conditions with a cesium-vapor triode. At higher cesium pressures, the oscillation period is an increasing function of the cesium pressure, which implies that the oscillations are controlled by scattering of positive ions in the interelectrode region. An approximate calculation of the ion accelerating voltage required to transfer ions from the middle of the emitter-collector space to the collector incicates a voltage of between 0.5 and 1.0 volt. This calculation is based on collisionless ion transport at low cesium pressures and ion transport dominated by charge-exchange collisions at high cesium pressures. It was observed that the oscillations stop at a definite point on the current-voltage characteristic.

Pulsed-discharge experiments were initiated to investigate current-density limiting factors in a cesium diode operating in the intermediate temperature range. The experimental technique consisted of applying a pulsed discharge to the test cell and observing the effect upon output current after the pulse. When the diode operation was space-charge limited, a large increase in current was observed after the pulse; whereas if the current was nearly emission limited, only a small increase was observed. Reasonable agreement was obtained between the current density measured after a pulsed discharge and the saturated electron current density obtained from the literature. Measurements of the time required to establish equilibrium after the pulsed discharge provided information on the physics of cesium diode thermionic converters. A calculation based upon the experimental measurements indicates that charge-exchange collisions will control ion transport to the emitter or collector, where surface recombination will occur.

(over)

UNCLASSIFIED

I. Thermionic energy conversion
II. Kaplan, C.
III. Office of Naval Research
IV. Contract Nonr 3738(00)

UNCLASSIFIED

Calculations have been performed based upon a literature survey of charge exchange collisions and ion mobility in cesium vapor. Charge exchange collisions result in a slowing down of positive-charge transfer within or across the interelectrode volume. The exploratory measurements of this report, together with the calculations summarized in Appendix A, indicate that charge exchange collisions may play an important part in determining the current-limiting factors in cesium thermionic converters.

UNCLASSIFIED

UNITERMS
Thermionics
Energy
Ions
Arc
Electric

UNCLASSIFIED